# MAGNETOPHONON EFFECT IN LEAD SULPHIDE

A Thesis

presented by

Farouk Al-Watban, B.Sc.

to the

University of St. Andrews

in application for the Degree

of Master of Science

"To the Country.

To Mother, Isline, sisters and brothers for their inspiration and to the memory of my father".

## DECLARATION

I hereby certify that this thesis has been composed by me, that it is a record of my work and that it has not previously been presented for a higher degree.

The research was carried out in the School of Physical Sciences in the University of St. Andrews, under the supervision of Dr. D.M. Finlayson.

F.A.H. Al-Watban

## CAREER

I first matriculated in the University of St. Andrews in October 1973 after I obtained my B.Sc. Degree (1967) in the University of Baghdad, Baghdad, Iraq.

I was enrolled as a research student in the Department of Physics with a scholarship from the Ministry of Higher Education, Republic of Iraq, under Ordinance No. 12.

At the end of my first year of study I passed the postgraduate examination with commendation.

CERTIFICATE

I certify that Farouk Al-Watban, B.Sc., has spent six terms at research work in the School of Physical Sciences in the University of St. Andrews under my direction, that he has fulfilled the conditions of Ordinance No. 12, and that he is qualified to submit the accompanying thesis in application for the Degree of Master of Science.

_____

Research Supervisor

ACKNOWLEDGEMENTS

I wish to express my sincere thanks to my supervisor Dr. D.M. Finlayson for his guidance, encouragement and advice which greatly enhanced my understanding. I am also very grateful to the Ministry of Higher Education, Republic of Iraq for my scholarship without which the completion of this work would not have been possible.

I would like to express my gratitude to Mr. J. McNab for his help and co-operation in the technical aspects of my work.

My thanks are also due to Professor J.F. Allen, F. Evans, J. Rogers and I. Bukowska for their help.

Abstract

Magnetophonon resistance oscillations have been observed in samples of n-type PbS at $77^{o}K$. These oscillations arise from intra-valley scattering of electrons by longitudinal optical phonons between Landau levels when the optical phonon energy $\hbar\omega_{LO}$ becomes a multiple of the cyclotron energy $\hbar\omega_{c}$.

After corrections are applied for the phase shift arising from the variation in amplitude of the resonance peaks and the polaron effect, the "bare" band edge mass is found to be $0.082\ m_{o}$.

## Introduction

The magnetophonon effect was first predicted by Gurevich and Firsov in 1961. However, although the first experiments were carried out in 1963 by Shalyt et al, only in the last few years has a substantial amount of work been carried out. Consequently the relevant theory has not yet been included in standard textbooks. For this reason, a summary of the original theoretical predictions followed by a simplified discussion of the physical basis of the effect will be given in chapters I and II.

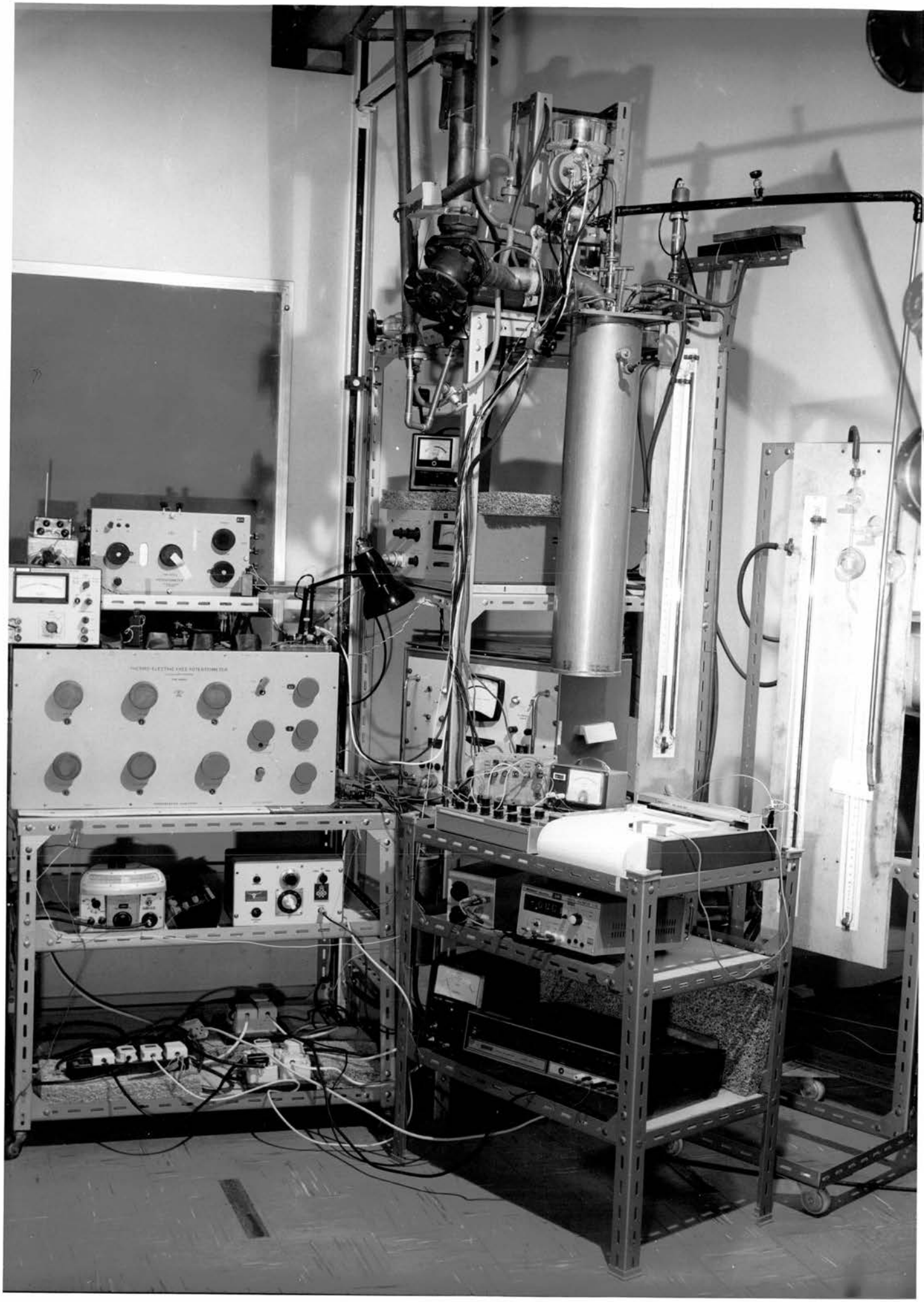

CONTENTS

# CHAPTER I

## 1.1 Prediction of the magnetophonon effect

A new type of transverse-resistivity oscillations in semiconductors in a magnetic field was predicted and studied theoretically in 1961 by Gurevich and Firsov. The oscillations are caused by inelastic scattering of electrons by phonons with limiting frequency different from zero, in particular, longitudinal optical phonons.

Gurevich and Firsov studied the influence of the inelasticity of the scattering on transport phenomena in a strong magnetic field. They restrict themselves to Boltzmann statistics [*a statistical distribution of a large number of electrons subject to thermal agitation and acted upon by magnetic and electric --- etc. fields. The number of electrons per unit volume in any region of the field, when the system is in statistical equilibrium is given by the equation* $N = N_o e^{-E/kT}$ *where* E *is the energy of the electron,* $N_o$*, the number of electrons per unit volume in a region of the field when* E *is zero,* k*, the Boltzmann constant,* T*, the absolute temperature of the system of electrons*] and use the Born approximation i.e. the energy of interaction of colliding particles is less than their kinetic energy.

In fact Argyres and Roth (1959) studied the inelastic scattering and obtained a formula for the transverse conductivity which was a sum over the electron quantum numbers in the magnetic field, by using the theory of electrical conductivity in a quantized magnetic field which was developed by Adams and Holstein, but they did not analyse this formula.

Éfros (1962) extended the theoretical investigation of Gurevich and Firsov to the case of Fermi statistics [*in which the number of electrons,* $n_i$*, in a state of energy* $E_i$*, at the absolute temperature* T*, is given by* $n_i = 1/(e^{(E_i-E_F)/kT} + 1)$] and predicted that a similar effect should also exist in degenerate semiconductors i.e. in semiconductors in which the number of electrons in the conduction band is so high that they

must be described by Fermi-Dirac statistics as in a metal.

These investigations were on the simplest semiconductor model, with a quadratic isotropic spectrum of carriers scattered by optical polar vibrators.

The aim of this survey is to give a qualitative understanding of these oscillations.

We shall consider the interpretation of the mechanism of transverse conductivity in a strong magnetic field i.e. $\omega\tau >> 1$ for each of the following cases.

1.1.1 Non-degenerate semiconductors

The Fermi energy $E_F$ can be defined as the energy at which the probability of occupation is 1/2. When $E_F << kT$ the Fermi-Dirac distribution function can be replaced to a good approximation, by the Boltzmann function. For such low electron densities we can also neglect electron-electron coulomb interactions.

When an electron of wave vector k is scattered by a phonon into the state $k'$, the electron either absorbs or emits a phonon of wave vector q where

$$k' = k \pm q \qquad \text{(conservation of crystal momentum)} \qquad [1\text{-}1]$$

In this process the electron either gains or loses a quantum of energy $\hbar\omega_q$. Conservation of energy for the system as a whole imposes the additional requirement

$$E' = E \pm \hbar\omega_q \qquad [1\text{-}2]$$

The scattering event can be considered quasi-elastic only if the energy change per collision is small compared to kT irrespective of the value of the Fermi energy.

Applying this to electron-phonon scattering, we conclude that

if $\Delta E < kT$ the process is elastic

and if $\Delta E > kT$ the process is inelastic.

Then: $\hbar\omega_q \approx k\theta_D$ $\theta_D$ is the excitation temperature of the phonon (Debye temperature)

$$kT << k\theta_D$$

or $$kT << \hbar\omega_q \qquad [1\text{-}3]$$

The phonon wave vector can take on magnitude ranging from q = o to

$$q_o = k\theta_D/\hbar u = [6\pi^3/V]^{1/3} \qquad [1\text{-}4]$$

where:

V is the volume of a unit cell

and u is the velocity of sound in the solid.

We use the Debye approximation in which the unit cell in wave-vector space is replaced by a sphere of equal volume. The wave-vector $q_o$ is, in fact, the radius of a sphere in k space whose volume is equal to that of the 1st Brillouin zone. Thus, absorption or emission of phonons can cause a significant change in the electron's crystal momentum [$|k'-k|$ *can be, and often is, the same magnitude as* $k_o$] but can change its energy by no more than $k\theta_D$, an energy increment very small compared to the Fermi-energy $E_F$.

For the inelastic scattering of electrons by phonons in non-degenerate semiconductors we can consider two characteristic cases:-

Case 1. Scattering by acoustical phonons.

This leads to a small effect because of very small phonon energy. We will eliminate this from our discussion since it is unrelated to our topic.

Case 2. Scattering by polar optical vibrators,

when account of the inelasticity may change all the characteristic dependences.

In calculating the conductivity of a semiconductor in which the constant energy surfaces are ellipsoidal, we must first calculate the current or conductivity contribution from a single ellipsoid and then sum over all the ellipsoids to obtain the total conductivity. Since the effective mass associated with each individual ellipsoid is a tensor quantity, so also is the conductivity. In general, the equations relating the current density and electric field may be written as tensor relations of the form

$$J_i = \sum_j \sigma_{ij} E_j$$

or [1-5]

$$E_j = \sum_i \rho_{ij} J_i$$

The $\sigma_{ij}$ and $\rho_{ij}$ are the elements of the matrix representing the conductivity and resistivity tensor of the crystal respectively. E is the electric field intensity, and J is the current density. If we deal with crystals having cubic symmetry, the conductivity tensor reduces to a scalar.

Choosing the z-axis to be along the direction of the magnetic field then in the case of an isotropic electron dispersion law, the tensor $\sigma_{ij}(B)$ has the form Parfenev et al (1974)

$$\sigma = \begin{pmatrix} \sigma_{xx} & \sigma_{xy} & 0 \\ -\sigma_{xy} & \sigma_{yy} & 0 \\ 0 & 0 & 0 \end{pmatrix}, \qquad [1\text{-}6]$$

$$\sigma_{xx} = \sigma_{yy}$$

The appropriate components of the resistivity tensor $\rho_{ij}(B)$ is the inverse of equations [1-6] which followed from [1-5]. In magnetic fields satisfying the condition $\omega_c \tau >> 1$, if the electron isoenergetic surface does not contain open orbits, the conductivity tensor $\sigma_{ij}(B)$ has the following asymptotic forms

$$\sigma_{xx} = \sigma_o(\omega_c\tau)^{-2}, \quad \sigma_{xy} \sim \sigma_o(\omega_c\tau)^{-1}$$

$$\sigma_{zz} \sim \sigma_o \qquad [1\text{-}7]$$

where $\sigma_o$ is the conductivity when H = 0.

The non-zero components of the resistivity tensor $\rho_{ij}$ are related to the components of the tensor $\sigma_{ij}$ in the following way:

$$\rho_{xx} = \frac{\sigma_{xx}}{\sigma_{xy}^2}, \quad \rho_{xy} = -\frac{1}{\sigma_{xy}} \qquad [1\text{-}8]$$

To make it possible to express $\sigma_{xx}$ and $\sigma_{xy}$ (the transverse and Hall conductivity respectively) as expansion powers of the scattering potentials, Gurevich and Firsov define a strong magnetic field as a field which satisfies the condition

$$\frac{\sigma_{xx}}{\sigma_{xy}} \sim (\omega_c\tau)^{-1} << 1 \qquad [1\text{-}9]$$

The range of strong fields includes the classical and the quantum region.

1.1.1a Scattering by optical phonons in quantum region

The quantum region is practically attainable if the following inequality holds

$$\frac{\hbar\omega_c}{kT} >> 1 \qquad [1\text{-}10]$$

where $\omega_c$ is the cyclotron frequency.

Here the quantum method is the only method which can be applied. Gurevich and Firsov found the dependence $\sigma_{xx}(B)$ for the case where:

$\omega_c >> \omega_{LO}$ where $\omega_{LO}$ is the longitudinal optical frequency and where the scattering is by acoustical and optical phonons.

This dependence is the same as the one obtained by Adams and Holstein (1959), apart from a logarithmic factor.

For $\omega_c << \omega_{LO}$ where Gurevich and Firsov could not use the method of Adams and Holstein they discovered a non-monotonic oscillatory dependence for $\sigma_{xx}(B)$. As in the classical case, $\sigma_{xx}$ goes through a maximum when the frequency $\omega_{LO}$ is a multiple of $\omega_c$, but what is a small correction in the classical case is part of the main effect in the quantum region.

By assuming that the electron dispersion law is quadratic and isotropic and that the magnetic field lies along the z-axis, and starting from Kubo's formula, which expresses $\sigma_{xx}$ in terms of velocity operators of the motion of the centre of the Landau oscillator. Gurevich and Firsov got after approximation and using suitable correction terms the following quantum formula

$$\sigma_{xx} = \sigma_{xx}^{el}[D + F(\alpha,\delta)] \qquad [1\text{-}11]$$

where

$$\sigma_{xx}^{el} = \frac{2}{3}\left(\frac{ne^2}{m^*\omega_c^2 t_o}\right)\left(\frac{\hbar\omega_{LO}}{kT}\right)\exp\{-\frac{\hbar\omega_{LO}}{kT}\} \qquad [1\text{-}12]$$

D: is a constant of order of unity, $t_o$ is a constant characteristic of the substance

$F(\alpha,\delta)$: is negligibly small compared to D if

$$\frac{\hbar\omega_c}{2kT}\,\delta(1-\delta) >> 1$$

But if

$$\frac{\hbar\omega_c}{2kT}\,\delta(1-\delta) << 1 \qquad [1\text{-}13]$$

$$F(\alpha,\delta) = -\left(\frac{3}{2}\sqrt{\frac{\hbar\omega_{LO}}{kT}}\right)\frac{\hbar\omega_c}{2kT}\,\mathrm{In}\left[\frac{\hbar\omega_c}{2kT}\,\delta(1-\delta)\right] \qquad [1\text{-}14]$$

$$\delta = \frac{\omega_{LO}}{\omega_c} - N_o \qquad \text{where } \omega_c = \frac{eB}{m^*}$$

$N_o$ is the largest integer contained in the ratio $\frac{\omega_{LO}}{\omega_c}$.

The first term in equation [1-11] is the same as the classical expression for the conductivity.

The second term in equation [1-11] describes the specific quantum resonance oscillations of the conductivity which can be noticed against the background of the classical term when

$$\frac{\hbar}{kT} |\omega_{LO} - N\omega_c| << 1 \qquad N \text{ is an integer.}$$

These oscillations are periodic in the reciprocal of the field. The origin of these oscillations can be understood as follows.

$$\text{If} \qquad \omega_{LO} = N\omega_c \qquad [1\text{-}15]$$

then electronic transitions involving the absorption or emission of a phonon are possible, during which the quantum number changes by N.

1.1.1b Scattering by optical phonons in classical region

$$\text{where} \qquad \frac{\hbar\omega_c}{kT} << 1 \qquad [1\text{-}16]$$

Although in this region the Boltzmann transport equation is applicable Gurevich and Firsov again use the quantum calculation for $\sigma_{xx}$.

It turns our that when the scattering is by optical phonons $\sigma_{xx}$ can oscillate and go through a maximum whenever the limiting frequency of the optical vibrations $\omega_{LO}$ is a multiple of the cyclotron frequency. These oscillations are periodic in the reciprocal of the field. In contrast to all other known types of oscillations of the static conductivity they occur in the case of Boltzmann statistics.

The conductivity in a strong field is related to the conductivity at B = 0, according to the transport equation by a simple order of magnitude relation for B = 0

$$\sigma = \frac{ne^2\bar{\tau}}{m^*} \qquad [1\text{-}17]$$

$\bar{\tau}$ is an average relaxation time for conduction electrons.

Gurevich and Firsov estimated from that $\sigma_{xx}$ which should yield the correct order of magnitude and the correct field and temperature dependence, which is

$$\sigma_{xx} \sim \frac{ne^2}{\omega_c^2 \bar{\tau}\, m^*} \qquad [1\text{-}18]$$

Gurevich and Firsov consider two regions of possible values for the electron energy E. In the first region $0 < E < \hbar\omega_{LO}$, and in the second $\hbar\omega_{LO} < E < 2\hbar\omega_{LO}$. Electrons in the first region can only absorb optical phonons, as a result of which they get into the second region.

The probability for such a process is proportional to

$$N_o \sim \exp(-\frac{\hbar\omega_{LO}}{kT}) \qquad [1\text{-}19]$$

They got for this region for $\sigma_{xx}$ a similar expression like equations [1-11] and [1-12] in the quantum region.

Note only that equation [1-14] which is valid in the quantum case when

$$\frac{\hbar\omega_c}{2kT}\,\delta(1-\delta) << 1$$

require in the classical region the inequality

$$\delta(1-\delta) << 1$$

and equation [1-14] contains not

$$\mathrm{In}[\frac{\hbar\omega_c}{2kT}\,\delta(1-\delta)]$$

but

$$\mathrm{In}[\delta(1-\delta)]$$

The ratio $\frac{\omega_c}{\omega_{LO}}$ is thus essentially the only parameter in the theory of the transverse conductivity caused by the scattering by optical phonons.

The quantity $\frac{\hbar\omega_c}{2kT}$, however is a parameter only in small ranges of changes in B near resonance.

If $\frac{\omega_c}{\omega_{LO}} << 1$, the main difference between the quantum and classical regions is that in the former case the oscillations are part of the main effect while in the latter they are small quantum corrections.

The studies by Gurevich and Firsov for the oscillations in the classical and the quantum regions were for the case of scattering by optical phonons in ionic crystals, but since this effect is caused by the presence of a limiting phonon frequency, it is independent of the details of the electron-phonon interaction and therefore it can be observed in the atomic semiconductors as well, such as germanium [*actually been observed in* n *and* P *type* Ge *Eaves et al (1970)*].

1.1.2 Degenerate semiconductors

In quantum mechanics when different states of motion correspond to the same energy level, the states are said to be degenerate. If $E_F >> kT$ the Fermi-Dirac distribution function in state i at the absolute temperature T

$$n_i = \frac{1}{e^{(E_i - E_F)/kT} + 1} \qquad [1\text{-}20]$$

will be = 1 for $E_i < E_F$

and = 0 for $E_i > E_F$

The gas is said to be degenerate, and only the particles in the range of energy levels of width kT about $E_F$ are available for conduction.

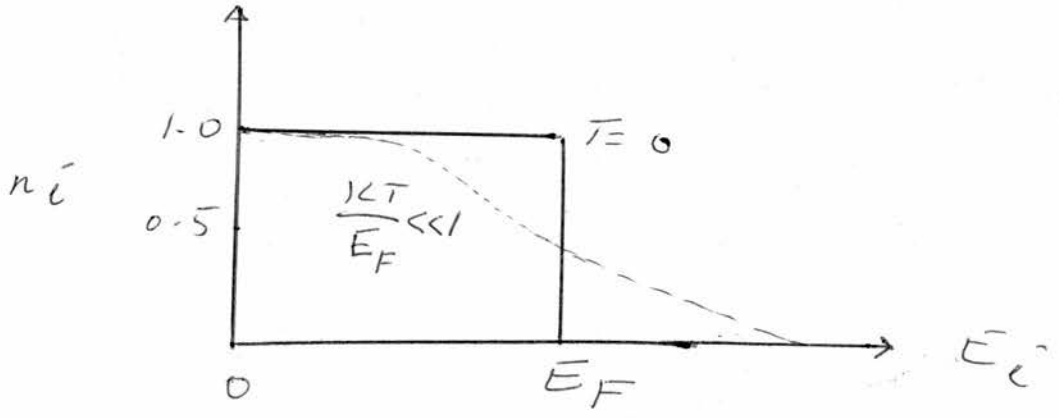

A degenerate semiconductor is a semiconductor in which the number of electrons in the conduction band is so high that they must be described by Fermi-Dirac statistics, as in a metal.

Efros (1962) considered this case, and he clarified the qualitative picture of the phenomena by a very simple consideration.

The contribution to the transverse electrical conductivity from the transition of an electron from a state with energy E to a state with energy $E + h\omega_{LO}$ is proportional to the density of initial and final states.

The density of states in a magnetic field becomes infinite if the longitudinal component of momentum $P_z$ (*the magnetic field is directed along the z-axis*) becomes zero, i.e.

$$E = h\omega_c(n + \tfrac{1}{2}) \qquad [1\text{-}21]$$

where $\omega_c = \frac{eB}{m^*}$.

If now $\omega_{LO}$ is a multiple of $\omega_c$,

$$\omega_{LO} = N\omega_c \qquad [1\text{-}22]$$

where N is an integer

then in a finite state $P_z$ may also equal zero and its energy

$$E + h\omega_{LO} = h\omega_c(n' + \tfrac{1}{2}) \qquad [1\text{-}23]$$

where $n' = n + N$.

In this case for a certain value of energy E the density of initial and final states becomes zero, as a consequence of which the electrical conductivity diverges logarithmically.

Thus oscillations periodic in $\frac{1}{B}$ arise with a period

$$\Delta\left(\frac{1}{B}\right) = \frac{e}{m^*\omega_{LO}} \qquad [1\text{-}24]$$

Again two cases are examined here the classical and the quantum limit.

1.1.2a Scattering by optical phonons in classical region

Here the classical region is defined by the inequality

$$E_F > \hbar\omega_c \quad . \qquad [1\text{-}25]$$

This means that many quantum levels will be occupied. In fact this region can show oscillatory effects like the Shubnikov de Haas effect (Putley 1960).

A quasi-classical region will be when

$$E_F >> \hbar\omega_c + \hbar\omega_{LO} \quad . \qquad [1\text{-}26]$$

For this condition Efros considered semiconductors with an isotropic and quadratic spectrum of electrons and again the criterion $\omega_c\tau >> 1$ satisfied, and for a magnetic field directed along the z direction.

He found that the oscillatory part of the conductivity when $J \perp B$ i.e. transverse conductivity is

$$\sigma_{xx}^{osc} = \frac{e^2 e \quad m^* A \ \omega_{LO}}{4\pi^3 \hbar^3 \ kT \ \omega_c} \ [-\hbar\omega_{LO}/kT] \ \text{In}\ \delta(1-\delta) \qquad [1\text{-}27]$$

Thus, a washing-out of the electrical conductivity is observed each time when $\omega_{LO}$ becomes an integral multiple of $\omega_c$. And the monotonic part of the electrical conductivity in this region in the limiting case $E_F >> \hbar\omega_{LO}$ is

$$\sigma_{xx}^{m} = \frac{2}{3} \ \frac{e^2 e \quad \omega_{LO} \ m^* \ E_F \ A}{h^4 \ \omega_c^2 \ kT \ \pi^3} \ [-\hbar\omega_{LO}/kT] \qquad [1\text{-}28]$$

where in both equations [1-27] and [1-28]

$$A = 4\pi^2 \hbar \left(\frac{Ze^2\gamma}{a}\right)^2 \ \frac{1}{Ma\omega_{LO}}$$

according to Davydov and Shushkevitch (1940)

or

$$A = 2\pi\hbar\omega_{LO} \ e^2 \left(\frac{1}{\epsilon_\infty} - \frac{1}{\epsilon_o}\right)$$

according to Krivoglaz and Pekar (1957)

Z: is the ionic charge

a: distance between neighbouring ions

$\gamma$: a dimensionless polarizability of the ion

M: the mass of a unit cell

$\epsilon_\infty$ and $\epsilon_o$ are the dynamic and static permittivities i.e. dielectric constant.

If we combine the oscillatory and the monotonic part we will get for the total conductivity (transverse)

$$\sigma_{xx} = \sigma^m_{xx}\left[1 + \frac{3}{8}\ \frac{\hbar\omega_c}{E_F}\ \ln\ \delta(1-\delta)\right] \qquad [1\text{-}29]$$

where $\frac{\omega_{LO}}{\omega_c} = 1 + \delta$

$\delta$ varies between zero to unity.

Just as for the Shubnikov-de Haas oscillations, the monotonic term differs from the oscillatory term by a factor of $\frac{E_F}{\hbar\omega_c}$. The essential difference is that this equation contains an exponential factor $e^{\frac{-\hbar\omega_{LO}}{kT}}$ due to scattering by optical phonons.

1.1.2b Scattering by optical phonons in quantum limit

In this region

$$E_F < h\omega_c \qquad [1\text{-}30]$$

This means that only the lowest level will be occupied. Efros found that

$$\sigma_{xx} = \frac{e^2 e^{\frac{-\hbar\omega_{LO}}{kT}}}{(2\pi)^4 \hbar^2 \omega_c\ kT} \sum_n G_{on}(E_F)\phi_n \qquad [1\text{-}31]$$

where

$$\phi_n = 2\ \ln\left[\sqrt{E_F^*} - \tfrac{1}{2} + \sqrt{E_F^* + \frac{\omega_{LO}}{\omega_c}(n+\tfrac{1}{2})}\right] - \ln\left[\pm\left(n - \frac{\omega_{LO}}{\omega_c}\right)\right] \qquad [1\text{-}32]$$

Now if $\omega_{LO} = N\omega_c$

$\phi_n$ diverges logarithmically. As a consequence oscillations of transverse electrical conductivity periodic in $\frac{1}{B}$ also arise in this region.

V is normalised volume.

The function $G_{on}(E_F)$ will not effect the oscillation.

For the case $\omega_{LO} >> \omega_c$ the oscillation becomes indiscernible and so it is not of interest to us.

1.1.3 Alternative derivations of the theory

After the prediction of the magnetophonon effect by Gurevich and Firsov (1961) a large amount of experimental and theoretical work was carried out. We will outline some of the recent theoretical work which came to the same conclusion of Gurevich and Firsov (1961), Éfros (1962) and Gurevich et al (1963).

Yasevichyate (1974) based his analysis for the scattering by optical phonons on the quantum transport equation derived by Levinson under the assumption that the electron-phonon coupling is weak, in a homogeneous case and for a weak electric field E. In the classical magnetic field Yasevichyate reached the same conclusion that the transverse conductivity consists of the monotonic part and oscillatory correction which is small.

Polovinkin and Skok (1974) solved the linearized Boltzmann transport equation for the inelastic scattering of electrons by optical phonons in a classical magnetic field, with an isotropic parabolic band, in the strong field approximation $\omega_c\tau >> 1$. Polovinkin and Skok derived an equation for the transverse resistivity which is in agreement with the classical limit of the result obtained by Gurevich and Firsov (1961) in the limiting case of low T i.e. $kT << \hbar\omega_{LO}$.

They also derived an equation which coincided with the classical limit of the quantum calculation of Éfros (1962).

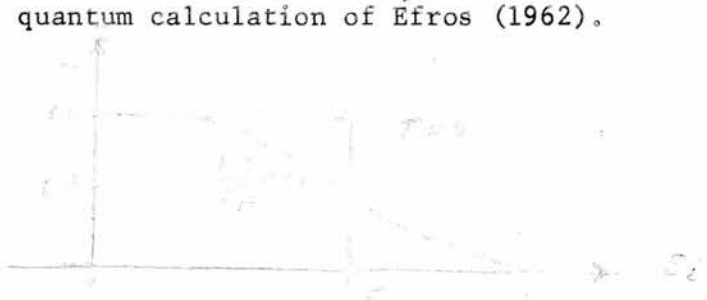

# CHAPTER II

## 2.1 Qualitative physical explanation of the magnetophonon oscillations

### 2.1.1 Classical picture of the transverse conductivity in magnetic field

According to the classical mechanics, electrons in crossed electric and magnetic fields describe their orbital motion with the cyclotron frequency $\omega_c$

$$\omega_c = \frac{eB}{m^*} \qquad [2\text{-}1]$$

m* is the effective mass which depends on the magnetic field orientation in the case of an isotropic carrier spectrum.

Simultaneously the centres of the circular orbits drift in the direction of the y-axis (*if* B *in z-direction, and* E *in x-direction*) with

$$V_y = \frac{E_x}{B_z} \qquad [2\text{-}2]$$

This drift is responsible for Hall conductivity.

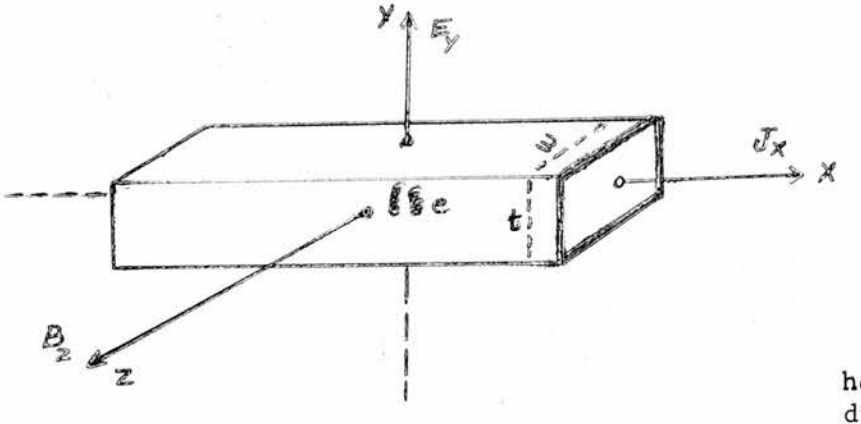



helical path of electrons drifting to y direction

$$\sigma_{xy} = \frac{ne}{B} \qquad [2\text{-}3]$$

The centre of cyclotron circles are not displaced along the x-axis. We may note that, the longitudinal electric field $E_x$ has to be precisely the same with or without a magnetic field. This result is no longer correct when the relaxation time $\tau$ is not constant, or the energy-band structure becomes anisotropic. It is then found that the longitudinal electric field will also depend upon the magnetic field

and ordinarily will increase, owing to the interaction with scatterers (*phonons, impurities, etc.*). This extra resistance arising from the addition of a magnetic field is called the magnetoconductivity or magnetoresistivity. Theoretically, calculating the conductivity or the current density is more convenient than the resistivity which is the experimentally measured parameter. The relation between the two is made clear in section (1.1.1).

## 2.1.2 Landau sub-bands

The interaction with the scatterers is defined by the time constant $\tau$. In every instance the most startling and precise results are obtained when the time constant (or relaxation time) of the charge carriers is long compared to the cyclotron period. We shall therefore, be principally concerned with this high field region, defined by the condition

$$\omega_c \tau = \frac{eB}{m^*} \tau >> 1$$

or [2-4]

$$\mu B >> 1$$

Consider a non-degenerate semiconductor, whose valence and conduction bands are parabolic and spherically symmetric in k space.

In the absence of a magnetic field the energies in the two bands are (Blatt 1968) and (Blakemore 1970)

$$\begin{aligned} E_n(k) &= E_c + \frac{\hbar^2}{2m_n} (k_x^2 + k_y^2 + k_z^2) \\ E_p(k) &= E_v - \frac{\hbar^2}{2m_p} (k_x^2 + k_y^2 + k_z^2) \end{aligned} \qquad [2-5]$$

However, we know that the application of a magnetic field $B_z$ will affect the motion of each electron in the x-y plane, while leaving motion along the z-direction undisturbed. The Lorentz force converts the electron motion into the sum of linear motion along the z-direction and cyclotron motion in the x-y plane. Thus an electron follows a helical path.

Landau described this by showing that the Hamiltonian operator of the Schrödinger equation has two additional terms when a magnetic field is present in the z direction. The motion in the plane perpendicular to H is quantized in a magnetic sub-band or a Landau level, while the motion remains continuous along H. The energies are now

$$E_n(k_z, n_c) = E_c + \hbar\omega_c(n_c + \tfrac{1}{2}) + \frac{\hbar^2 k_z^2}{2m_n}$$

$$E_p(k_z, n_v) = E_v - \hbar\omega_v(n_v + \tfrac{1}{2}) - \frac{\hbar^2 k_z^2}{2m_p} \qquad [2\text{-}6]$$

This situation, which is illustrated in Fig. (2-1) is startingly different from the uniform distribution of the electron states in k-space. We can see that the conduction bands are split into a series of one-dimensional sub-bands, each sub-band identified by the orbital quantum number n, which can take on only integral values. The minimum energy of the lowest, $n_c$ = o sub-band in the conduction band is raised to $\frac{1}{2}\hbar\omega_c$ and no longer zero. The sub-bands are separated by constant energy differences $\hbar\omega_c$ and this separation is independent of the other quantum number $k_z$. Quantization of the electron energy occurs not only for the simple dispersion law considered, but also in the more general case when the electrons undergo a finite motion over a closed trajectory in a plane perpendicular to the magnetic field.

The condition (2.4) means that in a strong magnetic field the spacing between Landau levels is much greater than the broadening of the levels that arises from oscillations. It is obvious that the fulfillment of this condition is necessary for the observation of all the effects associated with the quantization of the electron spectrum. In real crystals spatial inhomogeneities and the finite relaxation time will limit the definition of these states.

The inhomogeneity broadening may be reduced by choosing suitable samples. The relaxation broadening, at a given temperature, generally can not be reduced. Hence it is necessary to satisfy the inequality (2-4) for the magnetophonon oscillation. The Landau levels do not represent all of the final states available for the excitation in the crystal. There exist localized states near impurities and imperfections and also excitation states arising from the Coulomb attraction between a locally excited hole-electron pair. All these effects will screen the magnetophonon oscillation e.g. Firsov and Gurevich (1962) found that the electron interaction decreased the probability of the transitions.

2.1.3 Density of states in a magnetic field

Since according to equation [2-6], the electron energy depends only on the two quantum numbers n and $k_z$, each Landau sub-band is degenerate, the degeneracy being proportional to the magnetic field.

The magnetic field, as it were, collects states distributed uniformly over the band into discrete sub-bands. As a consequence of this, the density of states is also changed substantially

$$\Delta(E) = \left(\frac{2m}{\hbar^2}\right)^{\frac{1}{2}} \frac{1}{2\pi L^2} \Sigma (E-E_n)^{-\frac{1}{2}} \qquad [2-7]$$

where

$$E_n = (n+\tfrac{1}{2})\hbar\omega_c \qquad [2-8]$$

$$L = \left(\frac{\hbar}{eB}\right)^{\frac{1}{2}}$$ which is called the magnetic length.

The density of states Fig. (2-2) becomes infinite at the bottom of each Landau sub-band i.e. for $P_z = 0$, (*usually energy levels with* $P_z = 0$ *have been called simply Landau levels*).

2.1.4 Lattice vibration

The ions in a crystal are not stationary, but are, in fact vibrating about their equilibrium positions. The system behaves like an array of particles joined by harmonic springs. The classical

motion of such a system is the well known one of small oscillations and it may be described in terms of normal modes, i.e. independent motions of characteristic frequency. The problem of finding the normal modes and characteristic frequencies of a crystal is a classical one. The quantum mechanical description of the system is quite straightforward. Each oscillator will have its energy quantised with energy levels equally spaced at $(n+\frac{1}{2})\hbar\omega$.

n is the occupation number specified as a positive integer or zero for each type of oscillator. Even in the lowest energy state allowed by quantum mechanics (n=o), the energy of each oscillator is not zero but $\frac{1}{2}\hbar\omega$.

It is convenient to associate the concepts of a particle which we call a phonon with the quanta of vibrational energy. The situation is entirely analogous with the electromagnetic waves where the quanta are called photons.

If the oscillator passes from its nth to its (n+1)th state in a transition we say a phonon has been created (*or emitted*) in the process, and if passing from the nth to the (n-1)th state a phonon has been destroyed (*or absorbed*).

A lattice vibration is described by its frequency $\omega$ and its wave vector q, where the allowed values of q are in the first Brillouin zone.

The variation of $\omega$ with q i.e. the relation

$$\omega = \omega(q) \ , \qquad [2\text{-}9]$$

is called the phonon dispersion relation.

The phonon dispersion relation Fig. (2-3) has two branches, one called the acoustical branch because it has the typical characteristics of a sound wave, and the other the optical branch because of the similarity this frequency has to that of infrared light. As can be seen from the Fig. (2-3) the long wavelength optical modes [*which occupy the*

*region of q-space close to the origin*] are different from that of the acoustical modes in that they have a limiting frequency, and their group velocity $(\frac{d\omega}{dk})_{opt} \to 0$.

In general, a wave in a three-dimensional solid has both longitudinal and transverse character in both branches or modes. For the acoustic branch transverse and longitudinal

$$\omega(q) \to 0 \quad \text{as} \quad q \to 0$$

and the optical branch transverse and longitudinal

$$\omega(q) \to \text{constant} \quad \text{as} \quad q \to 0$$

Magnetophonon resistance oscillations occur with semiconducting meterials when the free carrier mobility is limited by scattering from the longitudinal polar optical modes. This is the dominant scattering mechanism in most compound semiconductors over a wide range of temperature.

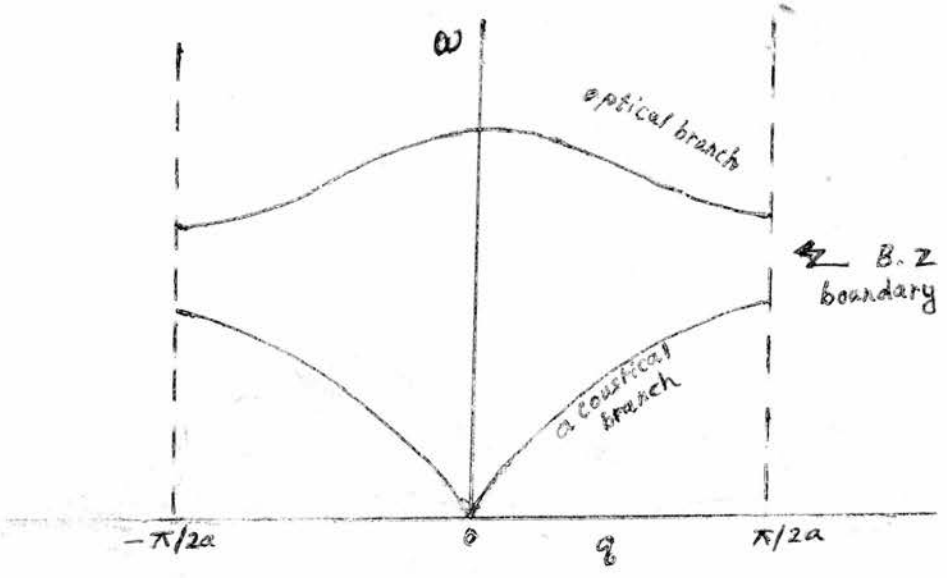


Fig. 2-3 Dispersion relationship for the propagation of a longitudinal wave in a linear diatomic lattice.

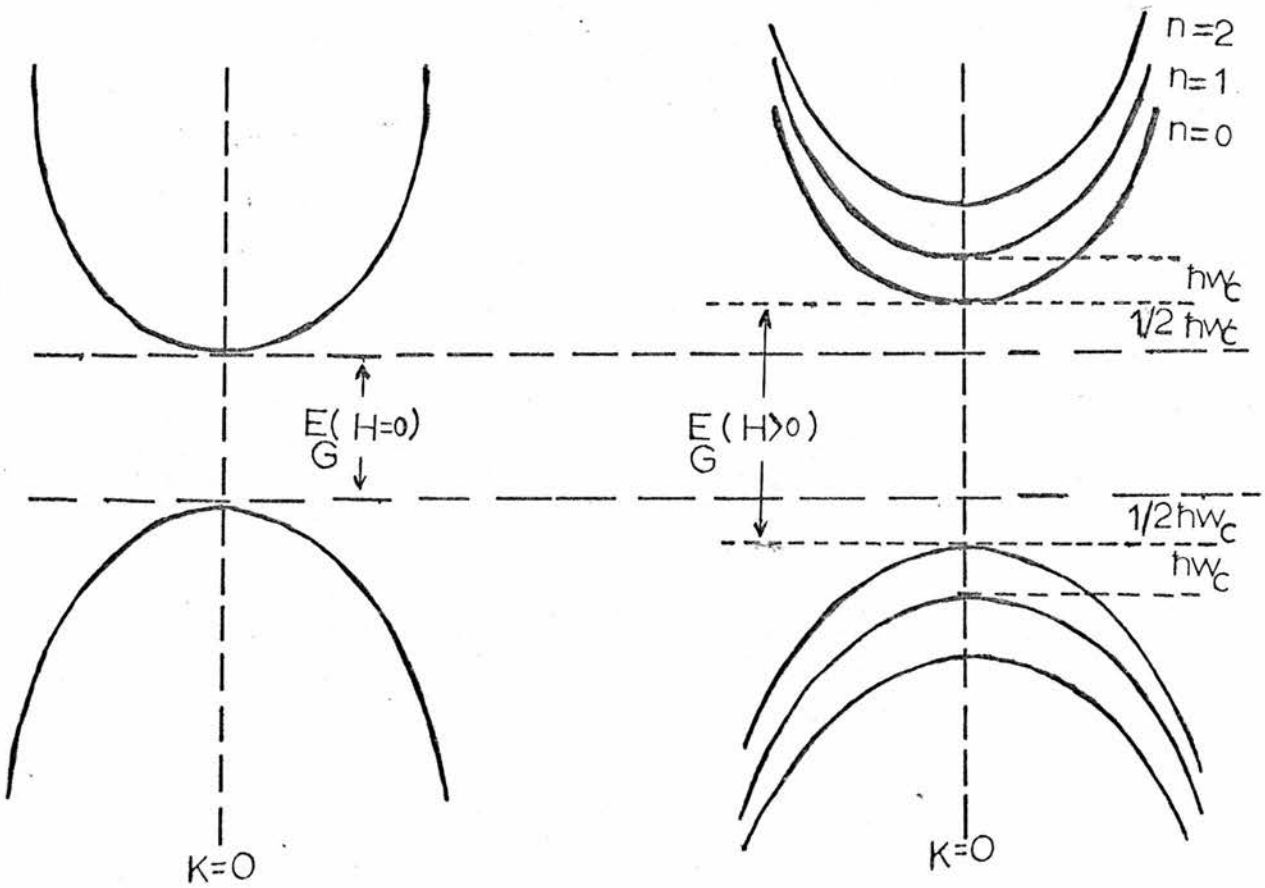


Fig.2-1. Energy bands for a simple semiconductor for H = 0 and H > 0

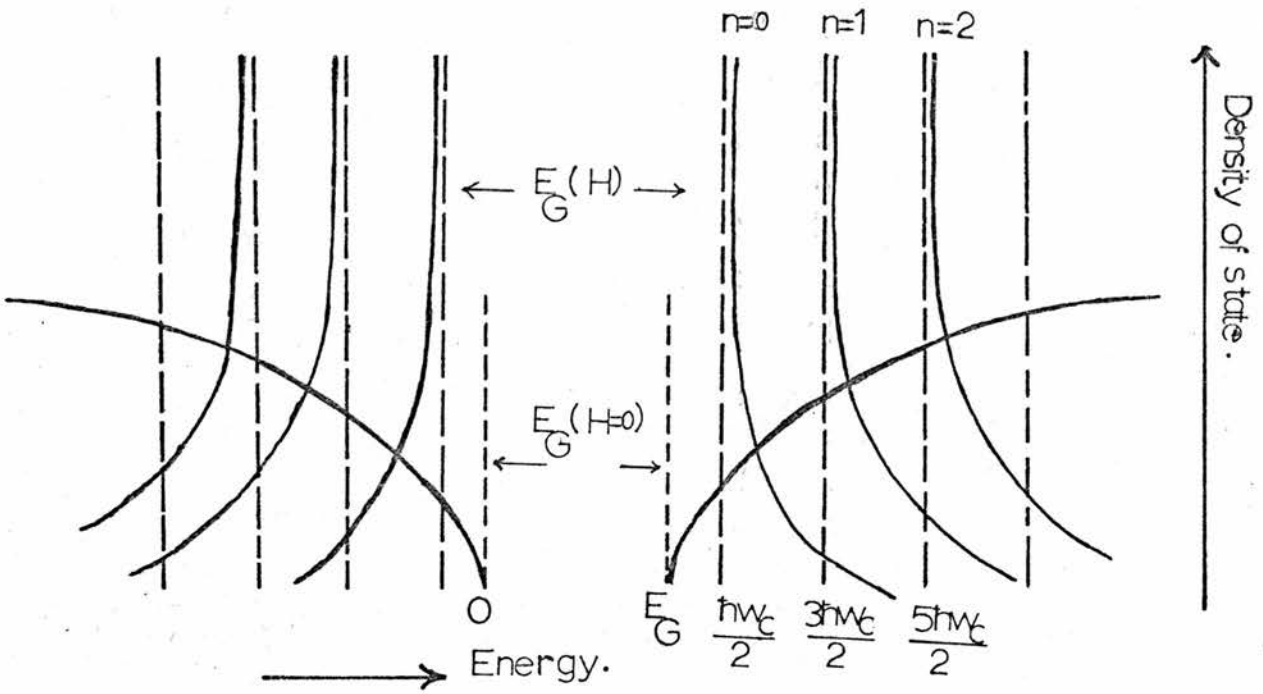


Fig2-2. Density of state in a simple semiconductor for H = 0 and H > 0

In the ionic crystal (*like* Pbs) there is a large splitting between the transverse and longitudinal optic branches. This apparently persists up to q = o. This splitting is due to the Coulomb forces and is related to the dielectric constant (Elliott 1974).

2.1.5 The Magnetophonon Resonance Oscillation (MPRO)

Physically the oscillations under consideration are caused by the peculiar course of the curve of density of electronic states in a magnetic field Fig. (2-2) [Gurevich et al 1963].

When $E \to \hbar\omega_c(n+\frac{1}{2})$ in equation [2-7] from the side of larger values, the density of states forms a sharp peak, approaching infinity like

$$\frac{1}{\sqrt{E - \hbar\omega_c(n+\frac{1}{2})}} \qquad [2\text{-}10]$$

Oscillation maxima are observed when transitions between two such peaks with phonon absorption or emission are possible. As a result of such [*represented by an arrow 1 in Fig. (2-4)*], an electron forms a state with energy E close to $\hbar\omega_c(n+\frac{1}{2})$, i.e. with a very low value of $P_z$ (*section 2.1.2*) and with another discrete quantum number

$$n' = n \pm M \qquad [2\text{-}11]$$

the absorbed or emitted phonon having the energy $\hbar\omega_{LO}$.
Such transitions are possible only if $\omega_{LO}$ is close to $M\omega_c$

$$\omega_{LO} = M\omega_c \qquad [2\text{-}12]$$

M is an integer 1,2,3 ---- etc.
Knowing that the magnetophonon oscillations are due to the discontinuous character of the density of states in its energy dependence.

The oscillation maxima of $\rho_{xx}(B)$ should occur when electron transitions between two Landau levels with absorption or emission of

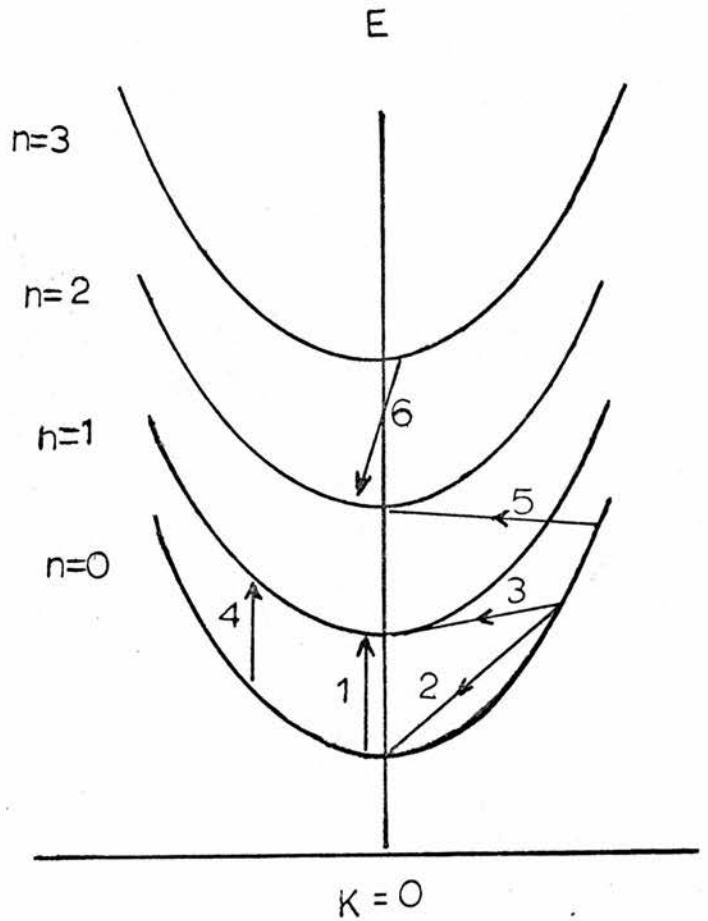


Fig. 2-5.

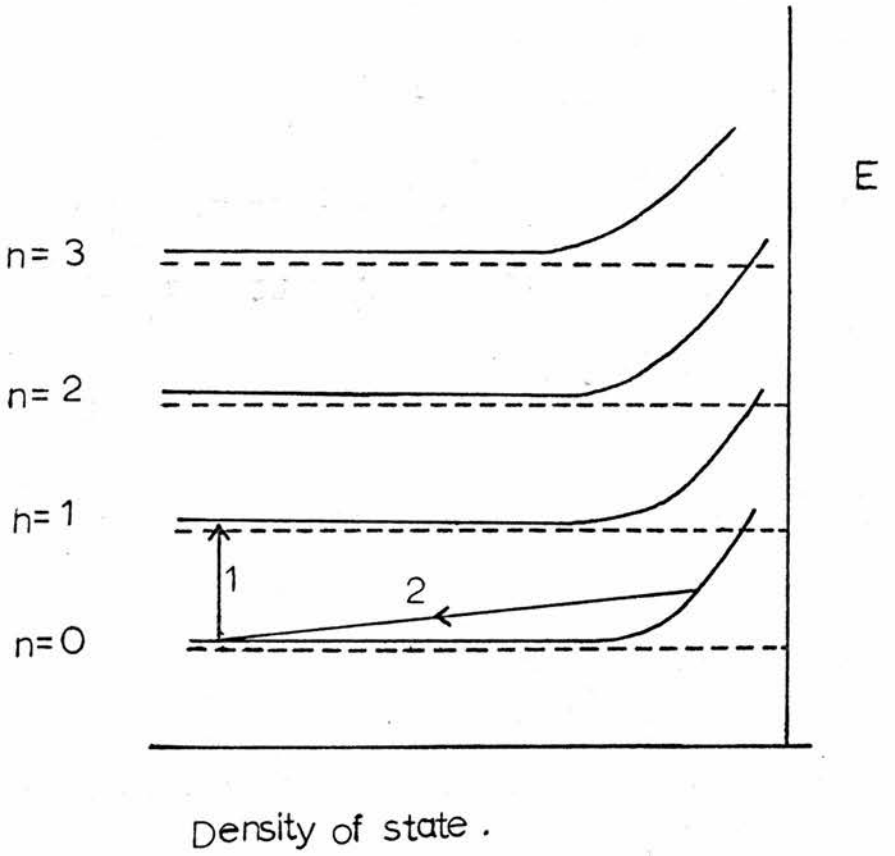


Fig 2-4.

an optical phonon $\hbar\omega_{LO}$ are possible.

For the first resonance M = 1 the possible transitions are shown in Fig. (2-5) by the arrow 1, in general, for the oscillating effect to appear as a non-monotonic variation. Variation of some of the quantities characterising both the initial and final states is necessary.

Therefore, transition of, e.g. the type 2 in Fig. (2-5) make no contribution to the oscillating part $\rho_{xx}(B)$, since for these only the density of final states has a singularity.

Such transitions, and also transitions of the type 4, produce the non-oscillating "background" of the function $\rho_{xx}(B)$. In addition horizontal transitions of the type 3 and 5 in Fig. (2-5), associated with elastic scattering by acoustic phonons and impurities, make a contribution to the non-oscillating "background" of the magneto-resistance (Dingle 1952).

Since, in the lowest approximation in the interaction, the transverse conductivity $\sigma_{xx}(B)$ is proportional to the scattering probability, the different scattering mechanisms do not interfere, i.e. they make an additive contribution to $\sigma_{xx}$, [Parfenév et al 1974]

$$\sigma_{xx} = \sigma_{xx}^{opt} + \sigma_{xx}^{ela} \qquad [2\text{-}13]$$

where $\sigma_{xx}^{opt}$ is the non-monotonic part due to scattering of electrons by optical phonons, [1-14] and [1-27]
and $\sigma_{xx}^{ela}$ is a certain smooth function of the magnetic field, associated with the elastic scattering [1-12] and [1-28].

A theoretical estimation of the conductivity $\sigma_{xx}$ has been made by Gurevich et al (1963) depending on the data by Gurevich and Firsov (1961), and Éfros (1962) section [1-1-1] and [1-1-2] respectively, which in case of

1. Boltzmann statistics [*non-degenerate semiconductors*]

$$\text{for} \quad \frac{\hbar\omega_c \delta}{kT} << 1$$

$$\sigma_{xx} = \sigma^B_{xx}\left(1 + \tfrac{3}{4}\sqrt{\frac{\omega_c}{\omega_{LO}}}\sqrt{\frac{\hbar\omega_c}{kT}} \quad \ln\left(\frac{2kT}{\delta\hbar\omega_c}\right)\right) \qquad [2\text{-}14]$$

where $\sigma^B_{xx}$ is the monotonic part of the conductivity

$$\sigma^B_{xx} = \frac{4\alpha ne^2}{3m^*}\left(\frac{\omega_{LO}}{\omega_c}\right)^2 \frac{\hbar}{kT} \exp\left(-\frac{\hbar\omega_{LO}}{kT}\right) \qquad [2\text{-}15]$$

2. Fermi statistics [*degenerate semiconductors*]

$$\text{for} \quad E_F >> \hbar\omega_{LO} >> \hbar\omega_c$$

$$\sigma_{xx} = \sigma^F_{xx}\left(1 + \frac{3}{8}\frac{\hbar\omega_c}{E_F} \ln\frac{1}{\delta}\right) \qquad [2\text{-}16]$$

$$\sigma^F_{xx} = \frac{4\alpha e^2}{3\pi^2\hbar}\frac{E_F}{kT}\left(\frac{\omega_{LO}}{\omega_c}\right)^2 \sqrt{\frac{2m^*\omega_{LO}}{\hbar}} \exp\left(-\frac{\hbar\omega_{LO}}{kT}\right) \qquad [2\text{-}17]$$

$\alpha$ is a dimensionless constant which is characterises the electron-optical phonon coupling (polaron effect)

$$\alpha = \frac{e^2}{\hbar}\sqrt{\frac{m^*}{2\hbar\omega_{LO}}}\left(\frac{1}{\epsilon_\infty} - \frac{1}{\epsilon_o}\right) \qquad [2\text{-}18]$$

$$\delta = \left|M - \frac{\omega_{LO}}{\omega_c}\right| , \quad (M = 1,2,\text{---}) \qquad [2\text{-}19]$$

We note that $\rho_{xx}(B)$ (*transverse magnetoresistivity*) is usually measured in experiments. The oscillating parts of the $\rho_{xx}$ and $\sigma_{xx}$ are related by equation [1-8]

$$\rho_{xx} = \frac{\sigma_{xx}}{\sigma x^2 y}$$

The oscillations in $\rho_{xx}$ are periodic in 1/B, with the period

$$\Delta\left(\frac{1}{B}\right) = \frac{e}{m^*\omega_{LO}} \qquad [2\text{-}20]$$

The period of the oscillations depends on the effective electron mass m* and on the limiting frequency $\omega_{LO}$ of the optical phonons.

These oscillations are called magnetophonon (MP) oscillations. The above formulae given are exact for the case of a cubic crystal and an isotropic carrier spectrum; in all other cases they are merely order of magnitude estimates.

2.2 Amplitudes and periods of the magnetophonon oscillations of $\sigma_{xx}$

The expression of $\sigma_{xx}$ in section (2-1-5), equations [2-14] - [2-16] leads to infinite values of the oscillation maxima.

From a physical point of view, it is obvious that there always exists some suppression mechanism limiting the height of the oscillation peak. Among the possible mechanisms that suppress the amplitude of magnetophonon oscillations are:

1. Broadening of the Landau levels as a result of elastic collisions, which leads to smoothing of the singularities in the density of states. This is a very decisive factor in conditions when elastic scattering is dominant (impurity for example) (Barker 1972).
2. Broadening due to electron-electron interaction decreases the probability of transitions [Firsov and Gurevich 1962]. The role of the Coulomb interaction can become noticeable only at sufficiently high electron concentration.
3. The strong interaction of an electron with polar phonon leads to formation of a polaron, for $\alpha << 1$, the energy of the polaron is equal to [Frölich 1963], $\alpha$ defined in equation [2-18]

$$E = \frac{\hbar k^2}{2m}\left(1 - \frac{\alpha}{6}\right) - \alpha\hbar\omega_{LO} \qquad [2\text{-}21]$$

It can be seen from equation [2-21], that the polaron effect leads to increase of the effective electron mass and lowering the energy by $\alpha\hbar\omega_{LO}$.

4. Broadening of the Landau level n = 1 Fig. (2-5) also leads to the suppression of the magnetophonon maximum in the transverse conductivity in the region of magnetic field $\omega_c = \omega_{LO}$.

Dworin (1965) shows that, together with the suppression of the magnetophonon peak there occurs a small shift in the positions of the magnetophonon maxima in the direction of higher fields relative to the resonance values (*the polaron shift*), the renormalized mass for $\omega_c = \omega_{LO}$ is greater than the polaron mass

$$m_{pol} = m(1 + \frac{\alpha}{6}) \qquad [2\text{-}22]$$

$m_{pol}$: is the electron-polaron effective mass

m: is the bare electron effective mass determined from equation [2-21] (Parfenév et al 1974).

A search for a polaron contribution to the magnetophonon mass was made with the relatively polar material n-CdTe [Hears et al 1968]. Increase of the magnetophonon mass over the cyclotron resonance mass was discovered equivalent to an $\frac{\alpha}{3}$ polaron contribution

$$m_{MPR} = m_{cycl} (1 + \frac{\alpha}{3}) \qquad [2\text{-}23]$$

A correction for the non-parabolicity of the CdTe conduction band, reduces the polaron contribution to the magnetophonon mass to [Harper et al 1973]

$$m_{MPR} = m_{cycl} (1 + 0.8 \frac{\alpha}{3}) \qquad [2\text{-}24]$$

The quantitative theoretical explanation for this enhancement of the polaron effect by the magnetic field remains an interesting but unresolved problem in quantum transport [Hears et al 1968].

Palmer (1971) has made a theoretical investigation to show that the correction which must be applied to the magnetophonon mass derived from the M = 1 peak to obtain the low frequency is

$$m_{MPR} = m_{cycl} (1 + 0.73 \frac{\alpha}{3}) \qquad [2\text{-}25]$$

Eaves et al (1971) used Palmer's theoretical work. The optical polaron correction which must be applied to the observed magneto-

phonon mass to obtain the "bare" mass is

$$m_{MPR} = m_{bare} \left(1 + 0.83 \frac{\alpha}{2}\right) \qquad [2\text{-}26]$$

5. The amplitude of the magnetophonon oscillation of $\rho_{xx}$ also has a distinctive temperature dependence.

At a temperature much less than the excitation temperature of the optical phonons [$\theta_D = \frac{\hbar\omega_{LO}}{k}$], the main contribution to the conductivity is made by the elastic scattering processes.

An increase in temperature leads to an increase in the role of scattering of electrons by optical phonons, as a result of which the amplitude of the magnetophonon oscillation also increases. However, at temperatures comparable with the excitation temperature of phonons, thermal broadening of the Landau levels, i.e. thermal spread of the electrons over the Landau levels, becomes important.

The temperature dependence of the amplitude of the oscillation is non-monotonic. There exists a certain optimal temperature at which the amplitude of the magnetophonon oscillation is a maximum, this temperature which is less than the excitation temperature of phonons depends on the contribution of the elastic scattering processes to the total conductivity.

## 2.3 Conditions for observation of the magnetophonon effect

1. The requirement common to all quantum magnetoresistance experiments is that the Landau states be sharp and well defined; that is

$$\omega_c \tau >> 1$$

2. Magnetophonon effect should be observed in these semiconductors and at those concentrations and characteristic energies of carriers at which the non-parabolic character is unimportant, or else if the latter is pronounced, one must try to reach the quantum limit which is

$\hbar\omega_c >> kT$ in Boltzmann statistics

or

$\hbar\omega_c > E_F$ in Fermi statistics.

3. If the predominant scattering mechanism is optical phonons it will be large enough for the oscillation to be observed experimentally.

4. If other scattering mechanisms predominate, one must bear in mind that when condition $\omega_c\tau >> 1$ holds the contribution of all various mechanism to $\sigma_{xx}$ are independent and additive, equation [2-13], but will lower the probability of seeing the effect.

5. At sufficiently high electron concentration, particularly, as a rule, when $E_F \geqslant \hbar\omega_{LO}$ with Fermi statistics, the main contribution to the "background" comes from scattering by ionized impurities. This scattering, like scattering by acoustic vibrations, is elastic [*Shubnikov-de Haas oscillations may be associated with it at low temperatures*].

6. The relative importance of scattering of optical phonons increases with decreasing concentration of impurities [*and hence of conduction electrons*], and increasing temperature [*lower than* $\theta_D = \frac{\hbar\omega_{LO}}{k}$].

## 2.4 Calculation of Line shape and amplitude of the magnetophonon effect

Intensive investigations have been carried out on n-type GaAs [*Stradling and Wood 1968*] InSb [*Stradling and Wood 1968, Stradling et al 1970*] and InP [*Eaves et al 1971*] to determine the dependence of the amplitude of the peaks on the magnetic fields, temperature and impurity contents of the samples. They show that the oscillatory terms are well represented by the empirical relation

$$\frac{\rho_{xx}^{osc}}{\rho_o} \sim \exp\left(-\gamma \frac{\omega_{LO}}{\omega_c}\right) \cos\left(\frac{2\pi\omega_{LO}}{\omega_c}\right) \qquad [2\text{-}27]$$

where $\gamma$ is a constant which depends on the sample mobility and temperature.

A relation similar to [2-27] was obtained by Barker (1972) who considered Landau-level broadening associated with multiple scattering of slow electrons with $P_z = 0$ by impurity centres. His formula for the oscillating part of the transverse magnetoresistance is

$$\frac{\Delta\rho_{xx}^{osc}}{\rho_o} = \sum_{r=1}^{\infty} \frac{1}{r} \exp\left(-r \frac{\gamma\omega_{LO}}{\omega_c}\right) \cos\left(2\pi r \frac{\omega_{LO}}{\omega_c}\right) \qquad [2\text{-}28]$$

The quantity $\gamma$, which determines the amplitude of the magnetophonon peak depends on the coupling constant $\alpha$ and on the scattering amplitude at the impurity centre, and does not depend on the magnetic field.

According to Barker the broadening due to interaction of the electrons with impurity centres is the determining factor of n-GaAs.

Gurevich et al (1962) estimate the ratio $\sigma_{xx}^{osc}$ to the magnitude of the conductivity $\sigma_o^{ela}$, although their expression describes the general form of the temperature dependence of the magnetophonon oscillations but it was found by Stradling and Wood (1968) that it gives a poor fit to the observed variation with magnetic field and sample mobility. Gurevich et al relations are:

1. For Boltzmann statistics at $h\omega_c \ll kT$

$$\frac{\sigma_{xx}^{osc}}{\sigma_o} \approx \alpha \exp\left(-\frac{\hbar\omega_{LO}}{kT}\right) \left(\frac{\hbar\omega_{LO}}{kT}\right)^{3/2} \frac{\mu H}{c} \left(\frac{kT}{\hbar\omega_c}\right)^n \qquad [2\text{-}29]$$

$\mu$ is the carrier mobility at $H = 0$.

The power n is determined by the scattering mechanism.

n = 0 for scattering by impurity ions

n = 1 for scattering by acoustic phonons

n = 2 for scattering by acoustic phonons and non-ionized impurities.

2. For Fermi statistics at $h\omega_c \leqslant E_F$

$$\frac{\sigma_{xx}^{osc}}{\sigma_o} \approx \alpha \exp\left(-\frac{\hbar\omega_{LO}}{kT}\right) \frac{\hbar\omega_{LO}}{kT} \frac{\mu H}{c} \left(\frac{\hbar\omega_{LO}}{E_F}\right)^{3/2} \qquad [2\text{-}30]$$

## 2.5 Magnetophonon and Shubnikov-de Haas oscillations

With any elastic scattering mechanism, in the case of Fermi statistics another type of transverse-magnetoresistivity oscillations with peaks of logarithmic form - called Shubnikov-de Haas oscillations - may be observed. In this case the densities of the initial and final states increase sharply simultaneously when the Fermi level approaches the value $\hbar\omega_c(n+\frac{1}{2})$. The period of such oscillations is

$$\Delta\left(\frac{1}{B}\right) = \frac{2e}{\hbar}\,(3\pi^3 n)^{-2/3} \qquad [2\text{-}31]$$

In the magnetophonon oscillations, scattering may be markedly inelastic if $\hbar\omega_{LO} >> kT$, and then all electrons in the energy interval from $E_F - \hbar\omega_{LO}$ to $E_F + \hbar\omega_{LO}$ take part in creating the effect. As noted earlier the densities of the initial and final states increase sharply simultaneously in this case if $\omega_{LO}$ is close to $M\omega_c$ and the oscillation period equal to

$$\Delta\left(\frac{1}{B}\right) = \frac{e}{m^*\omega_{LO}} \qquad [2\text{-}32]$$

We shall consider here those characteristic features of magnetophonon oscillations which distinguish them from Shubnikov-de Haas oscillations.

1. Unlike the period of Shubnikov-de Haas oscillations the magnitude of the period of magnetophonon oscillation does not depend on the electron concentration.

2. The two types of oscillations should have fundamentally different temperature dependence.

The SH oscillations appear only at sufficiently low temperature

$$kT << \hbar\omega_c$$ and increase on cooling,

while MP oscillations can appear only, at not too low temperature, when the optical phonons are sufficiently excited, when $\hbar\omega_{LO} > kT$ the amplitude of MP is proportional to $\exp(-\frac{\hbar\omega_{LO}}{kT})$, i.e. it increases exponentially with temperature. Owing to this the MP should as a rule be observed at substantially higher temperature than

SH oscillations.

3. The MP oscillations can occur either with Boltzmann or Fermi statistics, where as SH oscillations can occur only with Fermi statistics.

4. With Fermi statistics the MP can occur even at the ultra-quantum limit $E_F < \hbar\omega_c \leqslant \hbar\omega_{LO}$, where SH oscillations are impossible.

## 2.6 Summary

A theoretical prediction of a new type of oscillation of the transverse magnetoresistance $\frac{\Delta\rho}{\rho_o}$, [*Gurevich and Firsov 1962*] section [1-1], which is due to the inelastic scattering of carriers, in particular scattering with the longitudinal optical phonons has been detected in various semiconductors [*Harper et al 1973 and Stradling and Wood 1968, Parfenev et al 1974, for early literature*]. The nature of this oscillation can be understood as follows, section [2-1]. In a very strong magnetic field $\omega_c\tau >> 1$ when $\hbar\omega_c > \hbar\omega_{LO}$ the interaction of electrons are relatively weak, on reduction of the field intensity $\hbar\omega_c = \hbar\omega_{LO}$, the probability of scattering on the optical phonons increases sharply and the component of $\sigma_{xx}$ becomes greater.

On further reduction of the field $\hbar\omega_c < \hbar\omega_{LO}$ i.e. we move away from the resonance condition the inelastic interaction with optical phonons periodically decrease and increase on each approach to resonance

$$\hbar\omega_{LO} = 2\hbar\omega_c,\ 3\hbar\omega_c,\ 4\hbar\omega_c \text{ --- etc}$$

and the resonance condition will be

$$\omega_{LO} = M\omega_c \qquad M = 1,2,3 \text{ ---}$$

M is an integer. Because it does not contain the quantum constant h this oscillation should be also observed in the classical region section [1-1] [*Shalyt et al 1963*].

The oscillatory correction is difficult to detect not only because it is small but also because the distance between the individual Landau levels are small in classical magnetic field.

So fulfillment of the condition $\omega_c \tau >> 1$ or what amounts to the same thing $\mu B >> 1$, $\frac{\sigma_{xx}}{\sigma_{yy}} << 1$, equation [1-9], is required to observe the oscillations which are periodic in 1/B with a period

$$\Delta\left(\frac{1}{B}\right) = \frac{e}{m^* \omega_{LO}}$$

This effect has been given the name of magnetophonon resonance since it is due to inelastic resonance scattering of electrons by phonons of a definite frequency; in particular by optical phonons whose dispersion can be neglected.

Magnetophonon resonance is the first example known to science of an internal resonance in a solid i.e. of a resonance in which internal vibrations of the solid, e.g. optical phonons are the perturbing agent and it differs in this way from external resonance [*cyclotron,--- etc*] in which the perturbing agent is an external oscillating electromagnetic field.

The experimental study of these oscillations is of interest in the first place, because it enables one to investigate electron interaction with optical phonons in various semiconductors. If the electron spectrum is known it enables one to find the limiting phonon frequency; if the electron spectrum is unknown and the limiting phonon frequency is known, this effect can be used to study the electron spectrum and in particular the band structure parameters. The effective masses obtained by this method have been determined with high accuracy comparable with the accuracy of optical and magneto-optical [*cyclotron resonance*] methods.

So we decided to study this phenomena in lead sulphide semiconductors, in order that we can obtain a fresh value of the effective mass.

# CHAPTER III

## 3. Lead sulphide semiconductor

PbS is one of the $A^{IV}B^{VI}$ semiconductors which are often referred to collectively as the lead sulphide group or the lead salts or lead chalcogenides. They are extremely interesting semiconductors and for more than twenty years, these solids have been the subject of considerable research effort, due in part to the technological importance of these materials as detectors of infrared radiation.

The lead sulphide group exhibits properties which are unusual and possibly unique, relative to other semiconductors. One of these is that the temperature coefficient $\frac{dE_o}{dT}$ of the minimum energy gap $E_o$ is positive while all other elemental or binary compound semiconductors exhibit negative values of $\frac{dE_o}{dT}$.

Also the static dielectric constants are unusually large when compared with values observed for other semiconductors.

### 3.1 Crystal lattice

PbS crystallizes in the rock-salt crystal structure, the fundamental space lattice (*Bravais lattice*) is face-centred cubic. The crystal structure is shown schematically in Fig. [3-1]. The lattice constant a at approximately $300^{o}K$ is 5.9362 Å.

### 3.2 The Brillouin zone

The reciprocal lattice of the face-centred cubic lattice is body-centred cubic. The first Brillouin zone for the face-centred cubic lattice is the truncated octahedron shown in Fig. [3-2] for an electron of Bloch wave function

$$\psi_k(r) = U_k(r) \exp[i(k.r)] \qquad [3\text{-}1]$$

k is the electron wave vector.

Fig. [3-2] shows several special points and lines exhibiting the symmetry properties.

## 3.3 Crystal Bonding and Ionicity

PbS is a polar semiconductor, by which is meant that the interatomic bonds are predominantly ionic in character [*see Dalven (1973), for earlier literature*]. Additional information on ionicity of PbS is obtained from a calculation [*Dalven 1971*] of the electron-optical-polaron coupling constant $\alpha$ for PbS using the weak-coupling approximation. The value of $\alpha$ at $77^{o}K$ = 0.33, and it is large relative to the values of III-V compounds. The calculated value of $\alpha$ for PbS is consistent with the strongly ionic character inferred from its rock-salt crystal structure.

## 3.4 Phonon Spectra

The phonon dispersion relation $\omega = \omega(q)$ may be studied experimentally using inelastic scattering data, or from infrared absorption (*or reflection*) spectra, from Raman scattering spectra and from electron tunnelling data. Phonon dispersion curves derived from inelastic neutron scattering data have been reported for PbS at $296^{o}K$ [*Elcombe 1967*]. Information about the frequencies of the q = o LO phonons in PbS has also been obtained from electron tunnelling data at $4^{o}K$ [*Hall and Racette 1961*]. Table [3-1] gives LO phonon frequencies derived from these references.

Table [3-1]

| wave vector coordinate | special point of B.Z | Temp $^{o}K$ | $h\omega_{LO}$ meV | $\omega_{LO} \times 10^{12}$ c/s | error | references |
|---|---|---|---|---|---|---|
| 0,0,0 | $\Gamma$ | 296 | 25.4 | 38.64 | ±0.15 | Elcombe (1967) |
| | | 4.2 | 26.3 | 39.95 | ±0.4 | Hall and Racette (1961) |
| 0,0,1 | X | 296 | 11.45 | 17.40 | ±.05 | Elcombe (1967) |
| $\frac{1}{2},\frac{1}{2},\frac{1}{2}$ | L | 296 | 29.48 | 44.799 | ±0.15 | Elcombe (1967) |

## 3.5 Band Structure

One of the most interesting aspects of research on the lead salts in the last decade has been the fruitful interaction of experiment and theory. During this period, the calculation of the band structure of PbS, has been an especially important part of the study of these semiconductors.

Several band structure calculations of these compounds are available in the literature. Dalven (1973) provides a summary and references to earlier work using augmented-plane-wave (APW) method [*Rabii 1968*], the orthogonalized-plane-wave (OPW) method [*Herman et al 1968*], the empirical pseudopotential method (EPM) [*Lin et al 1966*] and [*Kohn et al 1973*]--- etc. all show the valence band maximum and the conduction band minimum at the L point in the Brillouin zone i.e. a minimum direct gap at L point. At $77^{o}K$ the energy gap $E_o$ is 0.307 ± 0.003 eV calculated by Mitchell et al (1964) and there is a massive experimental evidence supporting this conclusion like magnetoresistance measurements [*Allgaier 1961*], de Haas-van Alphen studies [*Stiles et al 1962*], Peizoresistance measurements [*Finlayson and Stewart 1966*]--- etc.

It thus appears quite well established that the energy gap in PbS is direct at the L point, the experimental studies [*Allgaier, Finlayson*] also delineated the constant energy surfaces near the L point. The surfaces of constant energy and thus the Fermi surface for both electrons and holes are prolate spheroids of revolution.

The major axis of the spheroid is a [111] direction and its centre is at the L point as shown in Fig. [3-3] within the first Brillouin zone there are eight half-spheroids, or, equivalently, four complete spheroidal constant energy surfaces.

Spheroidal [*or ellipsoidal*] is a good approximation to the Fermi surface only for low carrier concentrations i.e., for wave vectors near the band edges.

The fact that the surfaces of constant energy are non-ellipsoidal for high carrier concentrations implies that the energy bands are non-parabolic at wave vectors away from the band edges [*Dalven 1973*]. By non-parabolic is meant that the energy is no longer a simple quadratic function of k.

The non-parabolicity of the energy bands in PbS has been investigated experimentally by an analysis of the thermoelectric power in a strong magnetic field [*Ravich 1971*]. Then the effective mass and non-parabolicity of both bands, within the framework of K-P theory, are defined by the interaction of electron and hole bands only. The energy dispersion law is of the form

$$\frac{h^2 k_\perp^2}{2m_\perp^*} + \frac{h^2 k_\parallel}{2m_\parallel^*} = \varepsilon\left(1 + \frac{\varepsilon}{\varepsilon_g}\right) \qquad [3\text{-}2]$$

This is a modified Kane model [*Kane 1956*].

## 3.6 Scattering Mechanisms

The mobility of electrons and holes is a measure of their velocity of drift in a unit electric field. It is a useful quantity for studying interactions of the moving carriers with the lattice since the temperature dependence of mobility reveals the nature of the scattering mechanisms present in the crystal.

The scattering of electrons or holes by the acoustical vibrational modes of the lattice leads to a $T^{-3/2}$ mobility law [*Scanlon 1959*], whereas scattering by ionized impurities in the lattice is associated with a $T^{3/2}$ law [*Conwell and Weisskopf 1950*].

Scattering by the optical vibrational modes of the lattice leads to an expression for the mobility which varies exponentially with temperature [*Petritz and Scanlon 1955*], [*Howarth and Sondheimer 1953*], and [*Davydov and Shushkevitch 1940*].

Defects, such as dislocations may also scatter electrons and holes. Dislocations may trap electrons, holes, or ions and behave

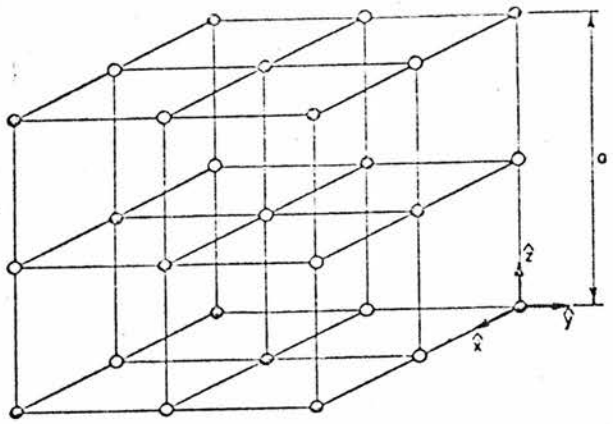


Rock salt (NaCl) crystal structure (schematic). The lattice constant of the conventional cubic unit cell is denoted by $a$. The unit vectors $\hat{x}$, $\hat{y}$, $\hat{z}$ in the three cubic directions are also shown.

Fig (3-1)

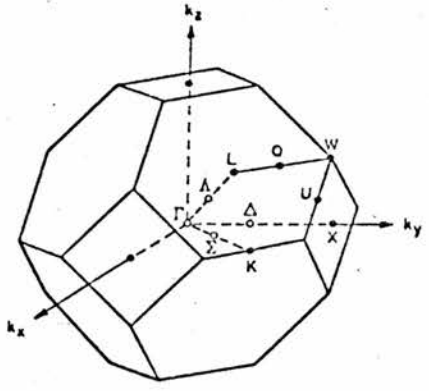


First Brillouin zone of the face-centered cubic lattice.

Fig (3-2)

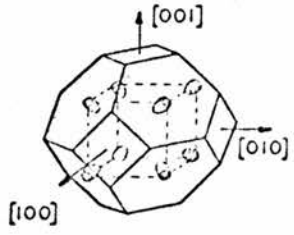


Brillouin zone of the lead salts showing the eight [111]-directed hemispheroidal surfaces of constant energy which contain the carriers (either electrons or holes). [T. E. Thompson *et al.*, *Phys. Rev. B* 4, 518 (1971).]

Fig (3-3)

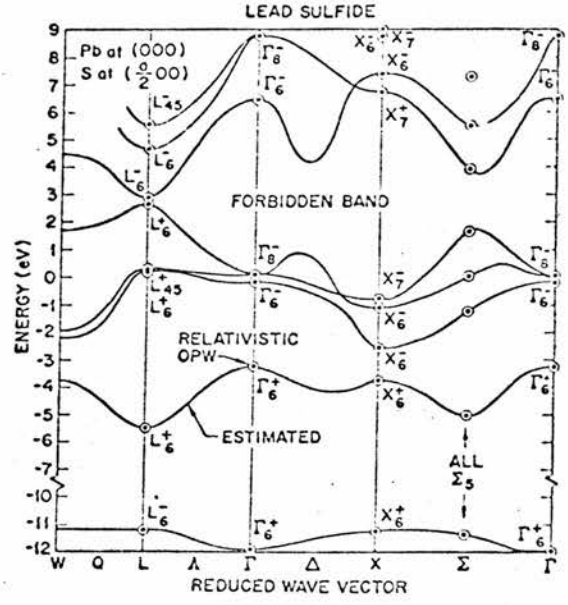


Fig (3-4)

Band structure of PbS calculated by the orthogonalized plane wave method. [F. Herman *et al.*, *J. Phys. (Paris)* 29, C4-62 (1968).]

like charged lines. These lines will be surrounded by cylindrical regions of opposite charge [*Scanlon 1959*]. Under these conditions the dislocation can have a relatively large effect in reducing the mobility, particularly at low temperature.

The behaviour of mobility has been approximated by the investigations, Putley (1952), Finlayson and Greig (1956), and Petritz and Scanlon (1955), by the formula

$$\mu = \mu_o T^{-n}$$

where n lies between 2 and 3, n = 2.2 given by Allgaier and Scanlon (1958).

Various theories of polar scattering [*Howarth and Sondheimer 1953*], [*Fröhlich and Mott 1939*], [*Low and Pines 1955*] predict a mobility which is proportional to the quantity

$$\sim \exp(+\frac{\theta}{T}) - 1$$

$\theta$ is Debye temperature.

The early investigations of the scattering mechanism in lead salts group were interpreted as follows, [*see Revich (1968) and Scanlon (1959) for early work*].

At a temperature higher than $100^{o}K$ the interaction with acoustical phonons is the dominant mechanism for carrier scattering in lead salts. While at low (*helium*) temperatures the scattering by the core impurity potential applies.

The interaction with optical phonons was rarely used to account for experimental data on lead salts though some papers contain the conclusion that the optical phonons play the appreciable role together with acoustical phonons [*see Ravich (1968) for these papers*].

Apart from that Howarth and Sondheimer (1953) discussed at length that in a polar semiconductor the high frequency optical modes may be at least as important as the acoustic modes in scattering the carriers

and they point out that at low temperature it is impossible to define a time of relaxation and hence the conventional expression for thermo-electric power cannot be obtained. Their calculations lead directly to rather complex formulae covering all ranges of temperature and degeneracy.

Finlayson and Greig (1958) in their measurement of the thermo-electric power of n-type single crystals of PbS showed that the simple theory, which considers scattering by acoustic modes only, fails to give agreement with experiment. The Howarth-Sondheimer theory of optical scattering fits the experimental results fairly well, suggesting that, over the temperature range considered, (*down to liquid hydrogen*) optical modes provide the dominant scattering mechanism.

Also Petritz and Scanlon (1955) suggested that the Howarth and Sondheimer theory may be valid for lead salts down to liquid nitrogen temperature.

Finlayson and Greig (1956) pointed out that the mobility varies with the impurity concentration and that at low temperature, lattice scattering, both acoustical and optical, is completely masked.

Kaidanov (1968) in his measurements of the Nernst-Ettingshausen effect, found that his values were closer to the predicted value for the optical scattering rather than to that for the acoustic scattering. Recently some pronounced advances has been made in investigations of transport phenomena and carrier scattering mechanism in lead salts. The experimental research and theoretical treatment of a variety of transport effects have been performed within a wide range of temperature and carrier densities [*see the Review article of Rauch 1971 part I and II*]. These show that:-

At temperature around $77^{o}K$ the consideration of polar optical phonon scattering is necessary in handling the experimental data, allowing a reasonable correlation with the theory at concentrations of about $10^{17}$ to $10^{18}$ $cm^{-3}$ [*the exact quantitative agreement is likely to be*

*impossible because of the significant divergence of the experimental data*].

At temperatures lower than about $10^{o}K$, the polar scattering is, indeed switched off since polar optical phonons cannot be excited. At sufficiently high temperatures the non-elasticity of polar scattering becomes evidently negligible. Thus use is made of the relaxation time approximation, showing that polar scattering is very important in general and becomes dominant at carrier concentration below about $4 \times 10^{18}$ $cm^{-3}$. In this region the polar optical phonon scattering makes the total mobility independent of concentration as follows from experimental research [*Ravich 1971(2)*].

In the temperature range around $4^{o}K$ scattering is mainly due to impurities and defects and scattering by phonons is of no significance. More recently Finlayson and Yau (1973) in their measurements of the electron mobility in high electric fields show a clear-cut decision regarding the relative importance of various scattering mechanisms. It appears that in PbS polar optical phonons provide the main scattering mechanism at $77^{o}K$ in fields up to 100 V $cm^{-1}$. At higher fields acoustic phonons play an increasing part. At present times one can ascertain the role of optical phonons in carrier scattering expecially at $77^{o}K$ and with a carrier concentration below some critical value $n_o$ which is about $1.1 \times 10^{19}$ $cm^{-3}$ for PbS [*Ravich 1971*].

This provided one of the reasons for investigation of the magneto-phonon effect in PbS.

The next important feature of the lead salts is that usually in a sample with a significant amount of free carriers present makes a consideration of screening effect essential.

This screening effect has direct influence on the transition probability. Moreover, they lead to an essential dispersion of optical modes in the long wavelength region, which is due to a large disparity between the values of $\epsilon_o$ and $\epsilon_\infty$ in these materials, and might lead to a change of the longitudinal optical frequency according to Ehrenreich (1959).

# CHAPTER IV

## 4. Experimental Techniques

### 4.1 Experimental Details

Samples of n-type PbS used in these experiments, have been selected from natural galena blocks. They were orientated along (100) direction and their average size was 6mm x 1mm x 1mm. Etching of these samples in thioureaic acid is necessary to remove oxidization.

The two ends of the samples were copper plated to ensure good electrical contact to the current leads by means of two beryllium copper pressure contacts [*see crystal holder* Fig (4-1)]. Pressure contacts were also used for the resistivity probes.

There was no injection of carriers because of the creation of a positive inversion layer between the metal and the n-type PbS semiconductor.

The homogeneity of these samples was checked by a probing method i.e. measurement of the resistance at short intervals.

The Carriers concentrations of these samples were determined by measuring the Hall effect at room temperature, and some of the samples were measured at Nitrogen temperature. There was no appreciable change of Hall Coefficient between the two temperatures. The Hall effect measurement was carried out in positive and negative magnetic field as well as positive and negative current.

An equation of the form

$$Vy = \tfrac{1}{2}\{\tfrac{1}{2}[Vy(+H+I) - Vy(-H+I)] - \tfrac{1}{2}[Vy(+H-I) - Vy(-H-I)]\} \qquad [4\text{-}1]$$

was then applied to get rid of the magnetoresistance which may appear due to an improper alignment of the Hall voltage probes.

The Hall Coefficient is defined as $R = J_x\ Bz/E_H$ and is equal to $\frac{3\pi}{8}\ \frac{1}{ne}$ for nondegenerate semiconductors.

### 4.1.1. Crystal Holder

This was designed by the author to fit the small experimental space for transverse and longitudinal measurement of magnetoresistance.

The sample was mounted onto the sample holder as shown in Fig [4-1]. The current leads were soldered to a pair of beryllium-copper sheets supported by a pair of nylon strips which could be moved to press on to the two ends of the sample.

The resistivity probes were made in a hook shape from beryllium copper wire soldered to one side of a beryllium copper sheet; which in turn is fixed by an adjustable screw for changing the contact pressure on the crystal. The otherside of the probes make a line contact with the sample.

The contactparts of the probes were cleaned and filed to make them like a knife edge for correct measurement of the distances.

The contact pressures of the probes was made adjustable by means of two screws to the current and two to the voltage probes. To ensure a minimum contact resistance, the resistance was measured by an ohmmeter and compared with the total resistance measured by the potentiometer.

Heat shrinkable sleeving was used to ensure a good contact between the beryllium copper wire and the surface of the crystal down to low temparature.

Close attention to the correct placement of the sample in the magnetic field was taken into account in the design of the crystal holder.

4.1.2. Magnetic field

A superconducting solenoid immersed in the liquid He supplied a magnetic field up to 40 Kgauss. This superconducting solenoid was driven by a super conducting magnet power supply unit which gave up to 21amperes, which is the maximum allowed current for the magnet. The magnetic field current was swept with respect to time linearly by an electromechanical sweep generator with a selection of speeds. This provides a continuous sweep from zero to maximum current and then back to zero again.

4.2. Method of measurement

Four different measuring techniques have been used and we shall discuss each of them in turn.

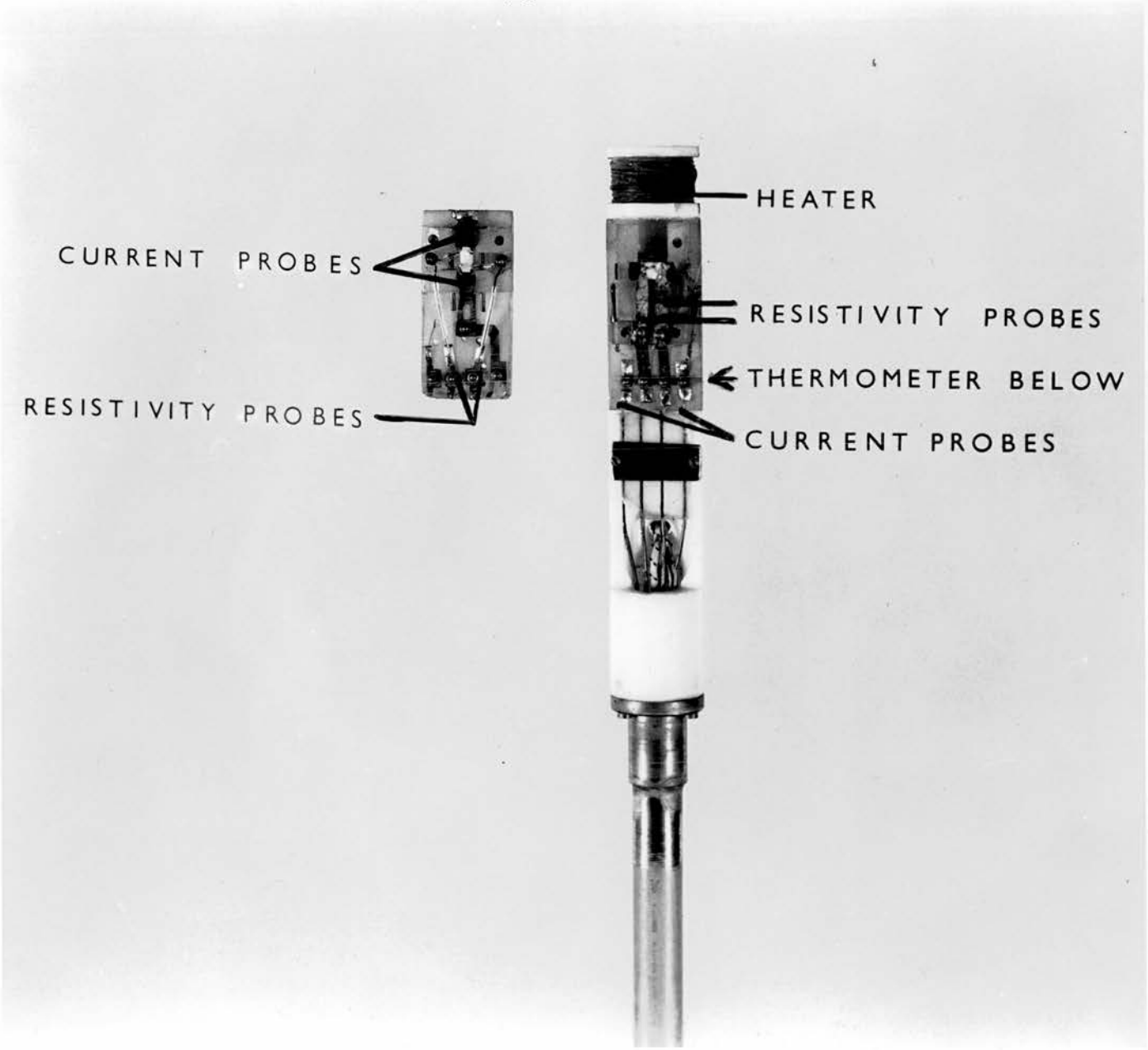
CURRENT PROBES
RESISTIVITY PROBES
HEATER
RESISTIVITY PROBES
THERMOMETER BELOW
CURRENT PROBES

4.2.1 Amplified Differential Technique

The signal from the sample was fed to a Diesselhorst potentiometer which balances the voltage at zero magnetic field. When magnetic fields are applied the unbalanced output from the Diesselhorst is amplified by a Keithley 149 milli-microvoltmeter and connected to two cascaded RC differentiating net works [Stradling and Wood 1970, Stradling 1972], and hence the Y terminal of X-Y Recorder (0.2 mv/cm); the X terminal of the X-Y Recorder was supplied from a constant [0.1 ohm] resistance in series with the current leads of the magnet. Details of the electrical connections are shown in Fig [4-2].

Constant current through the sample (10 m A) was provided by a constant current supply built in by the author Fig [4-2].

4.2.2. Direct Differential Technique

The signal from the sample was differentiated directly by means of two RC differentiator, without amplification, and fed to Kipp and Zonen single channel recorder type BD8 of 0.5mv full scale[20 cms scale], [*the circuit is similar to that shown in* Fig [4-2] *with the potentiometer and Keithley removed and the X-Y recorder replaced by the more sensitive Kipp and Zonen X-t recorder*].

4.2.3. Digitally Recorded Technique

A potential measurement was made point by point on a Diesselhorst potentiometer after amplifying the voltage by a Fluke model 845A high impedance voltmeter. [*As in* Fig [4-2]*with the Differentiator and the X-Y recorder removed and the Keithley replaced by the Fluke*],

4.2.4. Computerized Technique

A value was computed numerically from a digitally recorded $\rho$(B) & B data, using a six-digit DANA digital voltmeter Model 5330. [*as in* Fig [4-2] *with the Differentiator and the X-Y recorder removed, and the Keithley replaced by the Fluke for measuring the voltage of the sample. The current of the magnet was measured by digital voltmeter across the 0.1 ohm constant resistance*].

4.2.5. Thermometer

The temperature measurement was made by a GaAs diode thermometer which was calibrated by the author against platinum resistance to read from $1^{o}K$ to $300^{o}K$.

4.2.6. Cryostat

Since it was necessary to have a cryostat capable of maintaining a constant temperature over a wide range of temperatures we used a cryostat constructed by Yau (1971). This was designed to maintain a sample at $77^{o}K$ in the field of the superconducting magnet which was immersed in liquid helium. This was modified to give a temperature range from $4^{o}K$ to $250^{o}K$.

The assembly is showin in Fig[ 4-3 ]. The sample chamber consists of a vacuum jacketed stainless steel tube which fits into the inner cylinder of the magnet. The outlet F is connected to a diffusion pump to obtain a vacuum of better than 10 microtorr and the surfaces E of the jacket are polished to reduce radiation.

An exchange gas (He) through a needle valve B connected to the sample chamber, controls the quantity of the exchange gas. Below the sample holder G and thermometer K is placed a heater P of 100 ohm connected to a power supply. In operation exchange gas of about 3 torr is fed to the chamber and the vacuum jacket. Then the vacuum jacket evacuated to $10^{-4}$ torr. By means of heater P we could change the temperature from $4.2^{o}K$ up to $250^{o}K$ in steps and maintain to within $0.5^{o}K$ any temperature required in this range long enough to take a measurement.

4.3.0. Differentiator

The magnetophonon peaks are a very small fraction of the total magnetoresistance, therefore differential techniques are employed in order to eliminate the monotomic valuation of the resistance in recording of the magnetophonon effect. The differentiator is a two cascaded RC network [Stradling and Wood 1970, and Stradling 1972]. The response of the high-pass RC circuit to an input voltage increasing linearly with time is now to be considered.

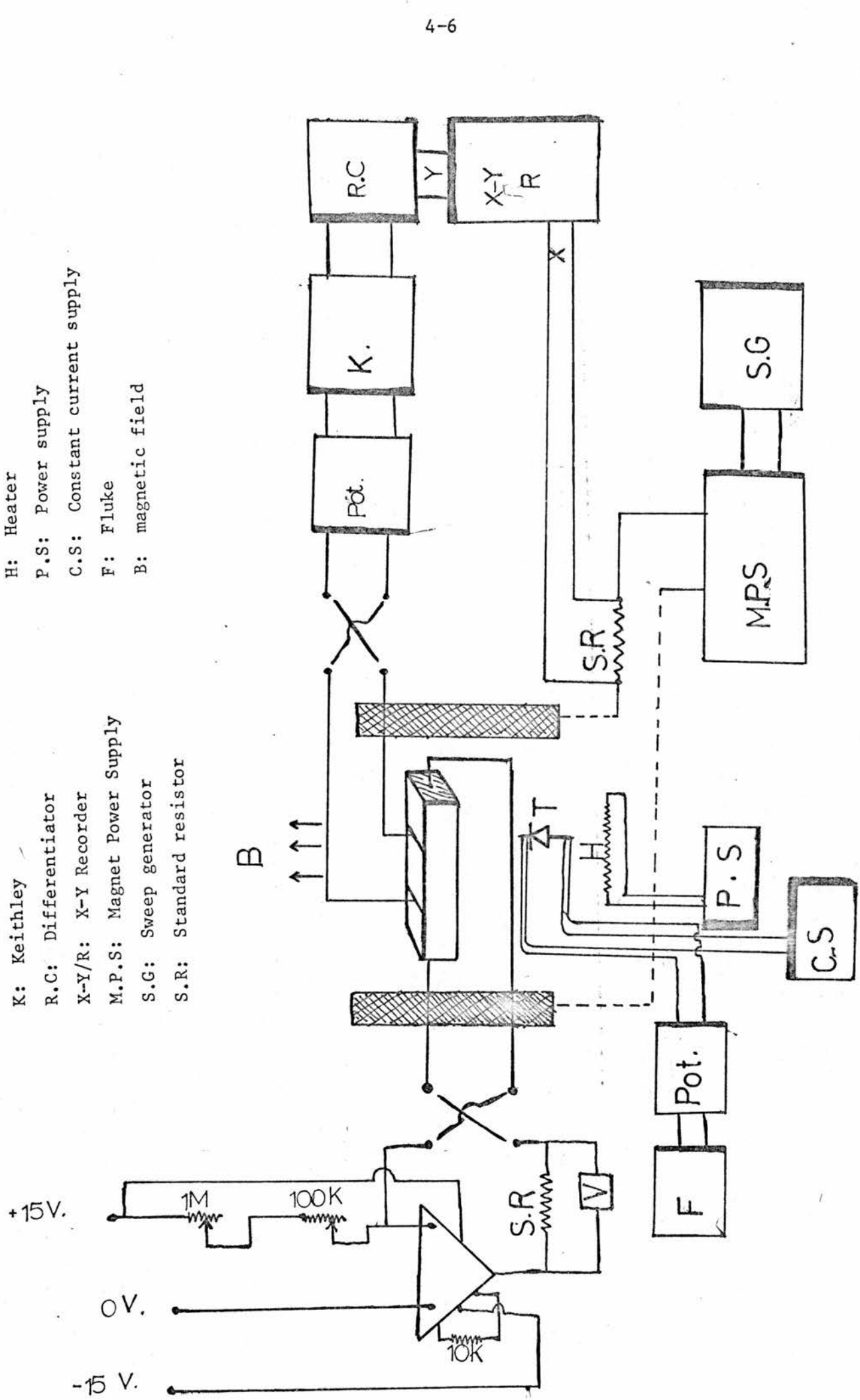
Pot: potentiometer
K: Keithley
R.C: Differentiator
X-Y/R: X-Y Recorder
M.P.S: Magnet Power Supply
S.G: Sweep generator
S.R: Standard resistor
T: Thermometer
H: Heater
P.S: Power supply
C.S: Constant current supply
F: Fluke
B: magnetic field
R.C
Y
X-Y R
X
K.
Pot.
S.G
M.P.S
S.R
B
T
H
P.S
C.S
Pot.
F
+15V.
1M
100K
S.R
V
0V.
10K
-15 V.

Fig. 4-2

E.L: electrical leads

R.P: rotary pump

B,F,E
G,K,P } see text section 4.2.6

N.T: Nitrogen Transfer

H.T: Helium Transfer

H.P: Helium Pump

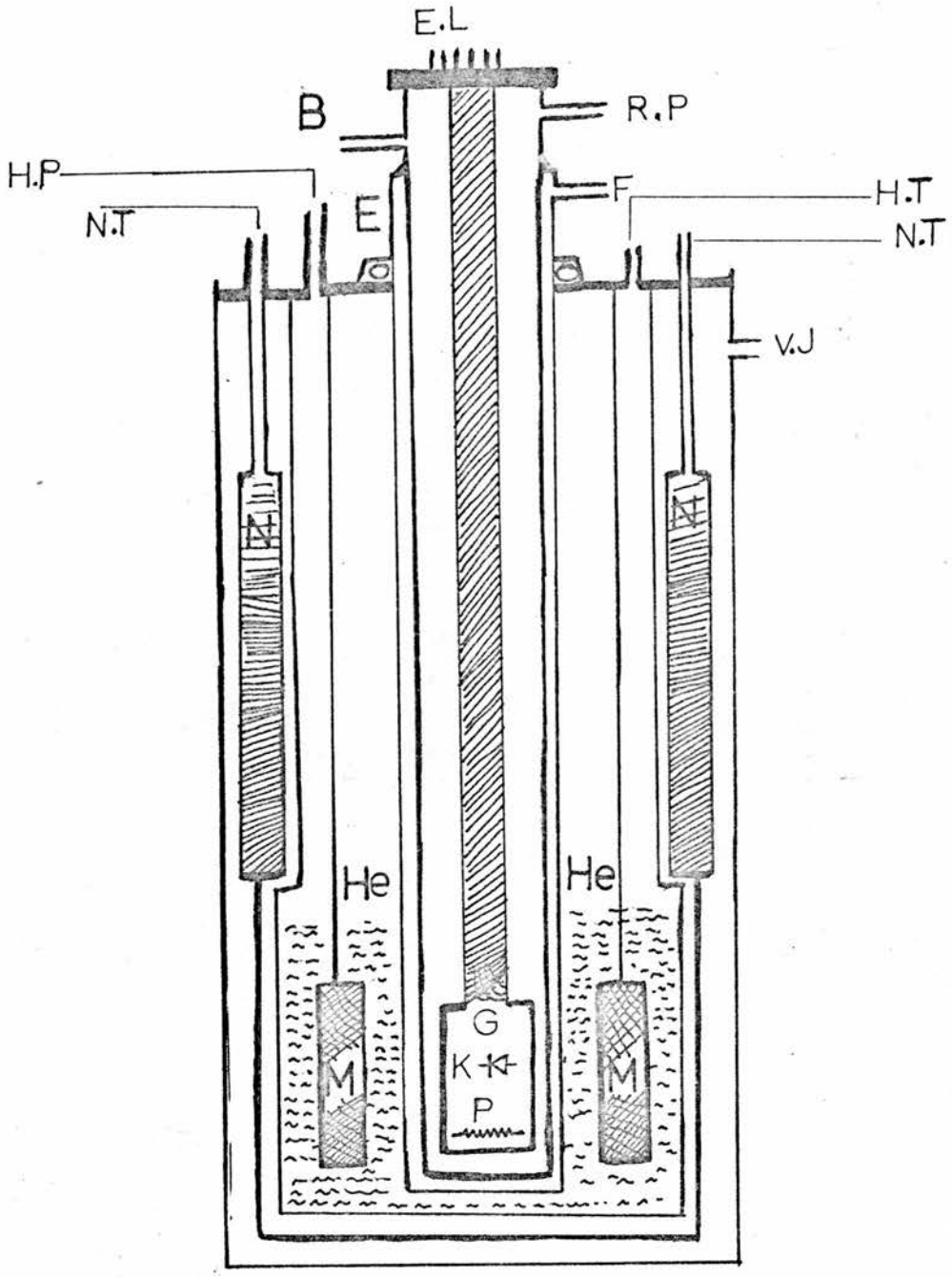


Fig. 4-3

The input voltage $V_i = \alpha t$, which is a function of time is called a ramp or sweep voltage. Such voltage is indicated as the "input" in Fig [4-5]. If this voltage is applied to the circuit of Fig [4-4], the output is governed by the equation

$$\frac{dVi}{dt} = \frac{Vo}{RC} + \frac{dVo}{dt} \qquad [4-2]$$

or

$$\alpha = \frac{Vo}{RC} + \frac{dVo}{dt} \qquad [4-3]$$

Equation [4-3] has the solution, for Vo = o at t=o,

$$Vo = \alpha RC \quad [1 - e^{-t/RC}] \qquad [4-4]$$

For times t which are very small in comparison with RC, we may replace the exponential in equation [4-4] by a series with the result

$$Vo = \alpha t \quad [1 - \frac{t}{2RC} + \ldots] \qquad [4-5]$$

The output signal falls away slightly from the input, as shown in Fig [4-5].

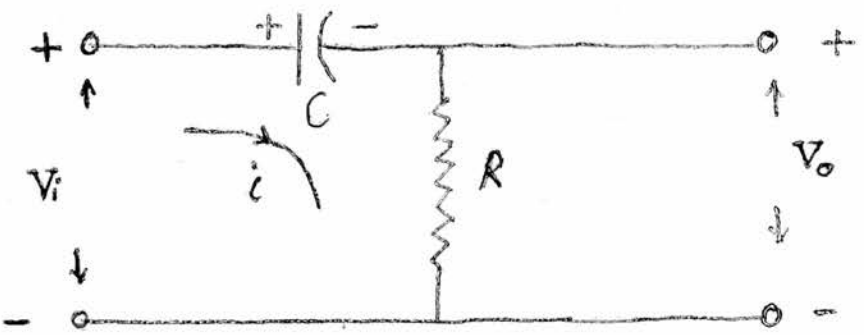


Fig. [4-4]

As a measure of the departure from linearity, let us define the transmission error $e_t$ as the difference between input and output divided by the input. For the error at a time t = T is then

$$e_t = \frac{Vi - Vo}{Vi} \approx \frac{T}{2RC} = \pi f_1 T \qquad [4-6]$$

Where $f_1 = \frac{1}{2\pi RC}$ is the low frequency 3-dB point. If in Fig [4-4], the time constant is very small in comparison with the time required for the input signal to make an appreciable change, the circuit is called a differentiator.

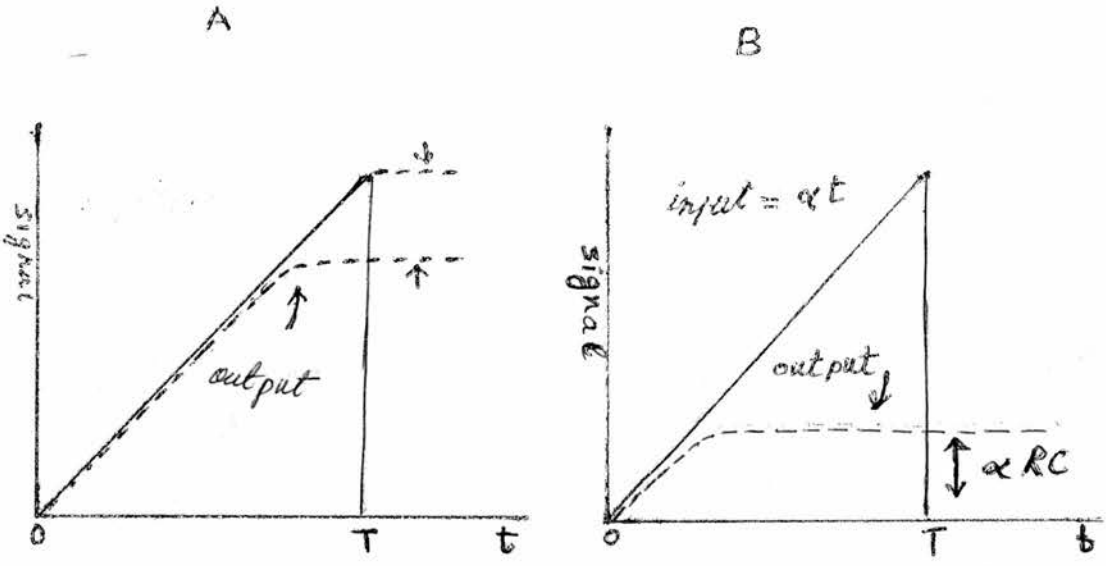


Fig[4-5] { A, Response of a high pass RC circuit to a ramp voltage for $\frac{RC}{T} >> 1$ ; B, Response to a ramp voltage for $\frac{RC}{T} << 1$ }

This name arises from the fact that under these circumstances the voltage drop across R will be very small in comparison with the drop across C. Hence we may consider that the total input Vi appears across C, so that the current is determined entirely by the capacitance.

Then the current is $C \frac{dVi}{dt}$, and the output signal across R is

$$Vo = RC \frac{dVi}{dt} \qquad [4-7]$$

Hence the output is proportional to the derivative of the input. For the ramp $Vi = \alpha t$, the value of $RC \frac{dVi}{dt}$ is $\alpha RC$. This result is verified in Fig [4-5] (B) except near the origin. The output approaches the proper derivative value only after a time has passed corresponding to several time constants, The error near t = o is due to the fact that in this region the voltage across R is not negligible compared with that across C.

It is interesting to obtain a criterion for good differentiation in terms of steady state sinusoidal analysis. If a sine wave is applied to the circuit of Fig [4-4], the output will be a sine wave shifted by a leading angle $\theta$ such that

$$\tan \theta = \frac{Xc}{R} = \frac{1}{\omega RC} \qquad [4\text{-}8]$$

and the output will be proportional to sin ($\omega t + \theta$). In order to have true differentiation we must obtain cos $\omega.t$. In other words, $\theta$ must equal 90°;this result can be obtained only if R = o or C = o. However, if $\omega RC = 0{,}1$, then $\theta = 84{,}3°$, and for some applications this may be close enough to 90°.

If two RC coupling networks are in cascade, and if the time constants $R_1C_1$ and $R_2C_2$are small relative to the period of the input wave, then this circuit performs approximately as a second-order differentiator.

The differentiator therefore suppresses the slowly varying components of the magnetoresistance and enables the approximately sinusoidal components to be displayed more readily. A distortion can happen in the recording and this is because the magnet current instead of the field is swept linearily. The time constant of the differentiator has to be determined accurately and is dependent on the speed of the sweep, so in order to obtain a reasonable approximation to the second derivative

$\frac{d^2\rho}{dB^2}$ which is the output of the two cascaded RC differentiators

[*The real output is* $\frac{d^2\rho}{dt^2}$ *not* $\frac{d^2\rho}{dB^2}$ *which can give another distortion*],

the time constant of the RC network should be much less than $\tau$, the magnetophonon oscillation period in real time at the chosen sweep rate. To have

$$RC \sim 0.1\ \tau \qquad [4\text{-}9]$$

is a reasonable approximation.

# CHAPTER V

## 5. Measurements

### 5-1 InSb

We first of all started with a sample of n-type InSb of carrier concentration $9 \times 10^{20}$ $m^{-3}$ and mobility about 37 $m^2 V^{-1} sec^{-1}$ of an approximate size of 5mm X 2.5mm X 1mm.

The Fermi energy for a degenerate semiconductor at absolute zero temperature $E_{Fo}$ is defined by

$$E_{Fo} = (3\pi^2 n)^{2/3} \frac{\hbar^2}{2m^*} .$$

For this sample

$$n = 9 \times 10^{20} \ m^{-3}$$

$$\hbar = 1{,}054 \times 10^{-34} \ \text{J.sec,}$$

$$m^* = 0{,}0145 \times 9{,}1085 \times 10^{-31} \ \text{Kgm at } 77^{o} \text{ K,}$$

[Smith et al. 1962 and Palik et al, 1961].

Then

$$E_{Fo} = 3{,}74 \times 10^{-22} \ \text{J.}$$

$$KT = 1{,}38 \times 10^{-23} \ \text{J.deg}^{-1} \times 77 \ \text{deg}^{-1},$$

$$\therefore \quad KT = 10{,}6 \times 10^{-22} \ \text{J.}$$

Hence since $KT > E_{Fo}$ this sample of InSb is non degenerate.

To examine the condition $\hbar\omega_c \geq kT$.

take B = 1Kgauss, then

$$\omega_c = \frac{eB}{m^*} = \frac{\text{coul.} \times 10^3 \times 10^{-4} \ \text{Kgm}}{\text{Kgm} \cdot S^2 \cdot A}$$

$$\omega_c = 12{,}1 \times 10^{11} \ sec^{-1}$$

and $$\hbar\omega_c = 12{,}8 \times 10^{-23} \ \text{J.}$$

So

$$\hbar\omega_c > KT$$

for fields larger than 8 Kgauss.

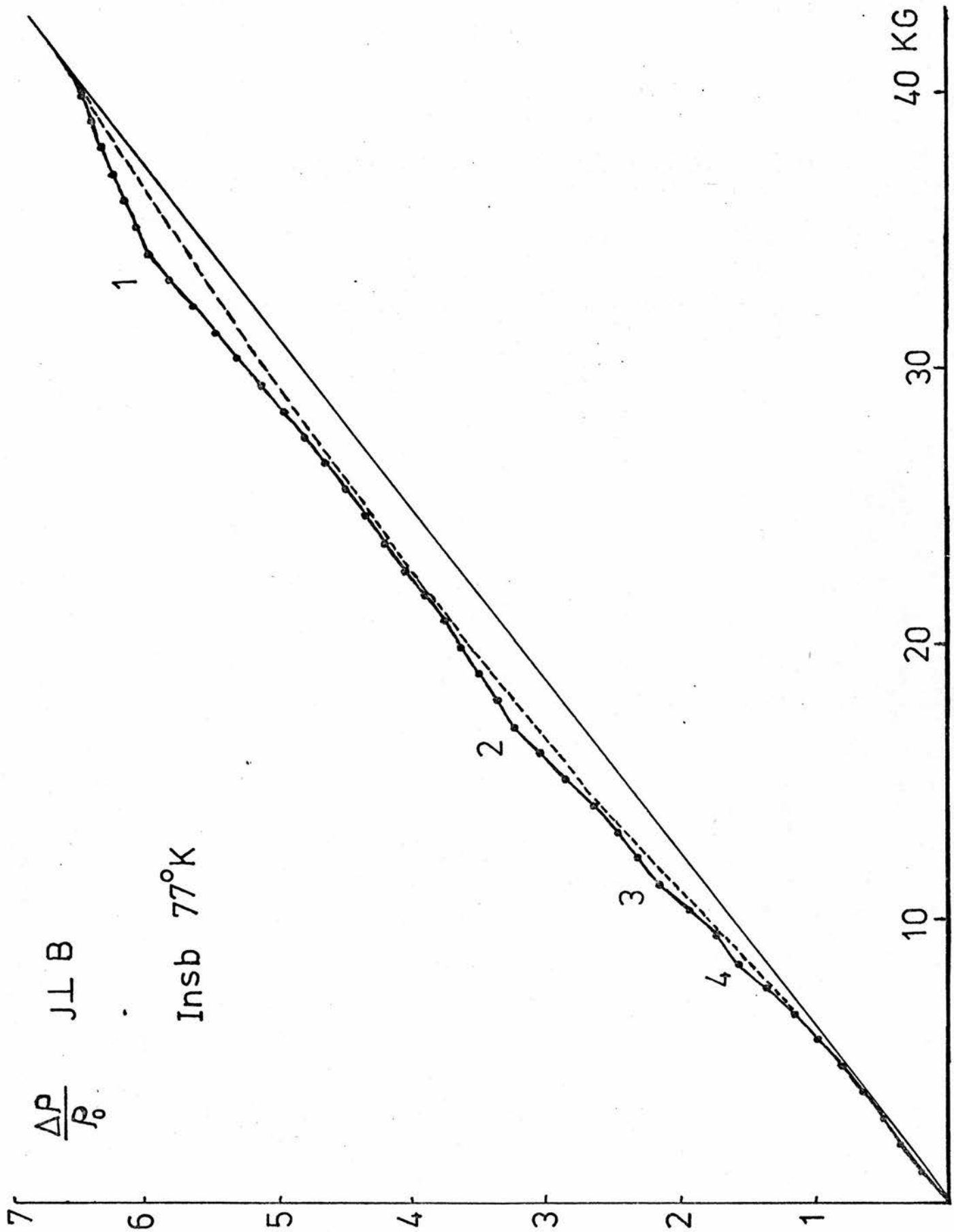


Fig. 5-1

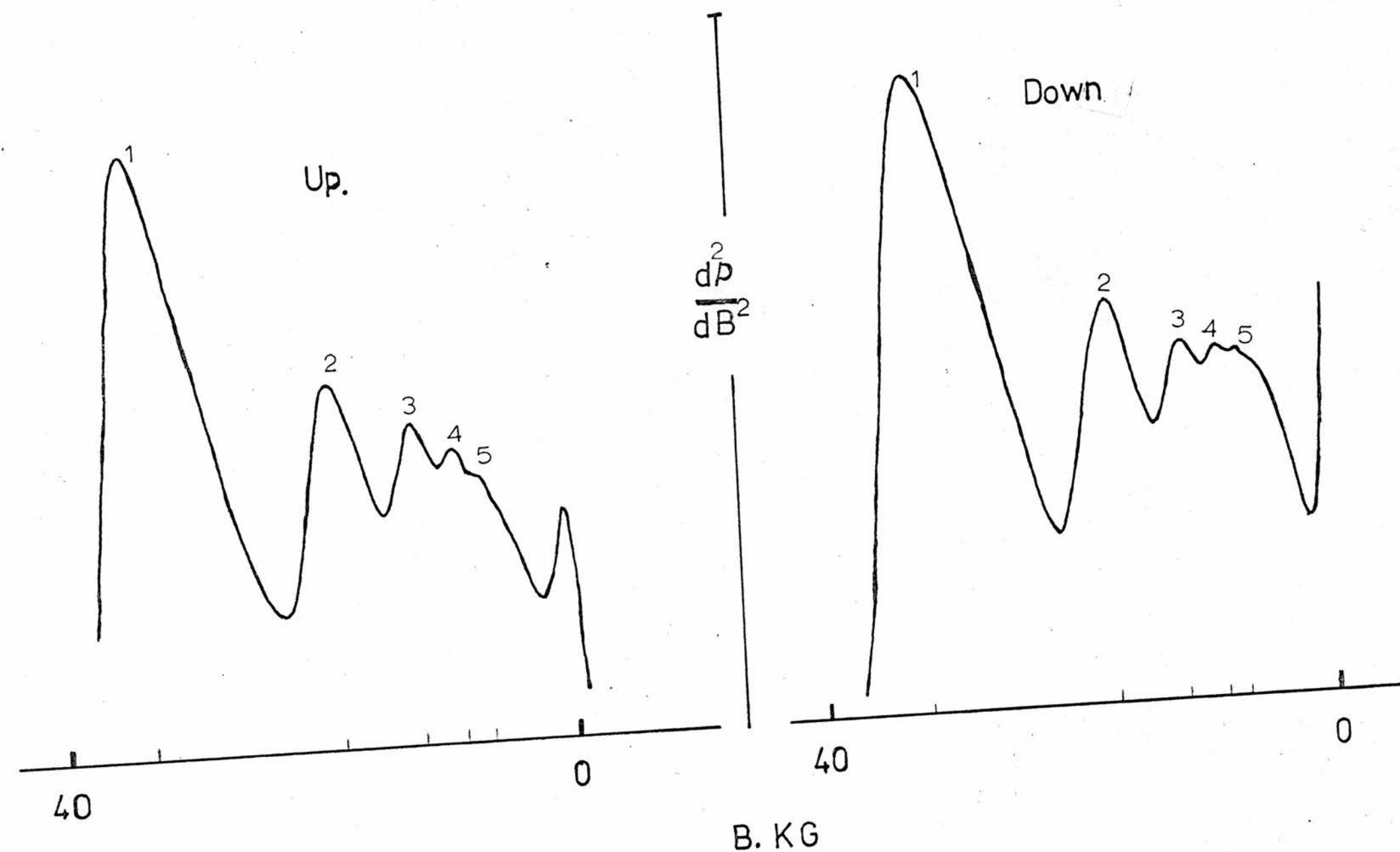


Fig. 5-2

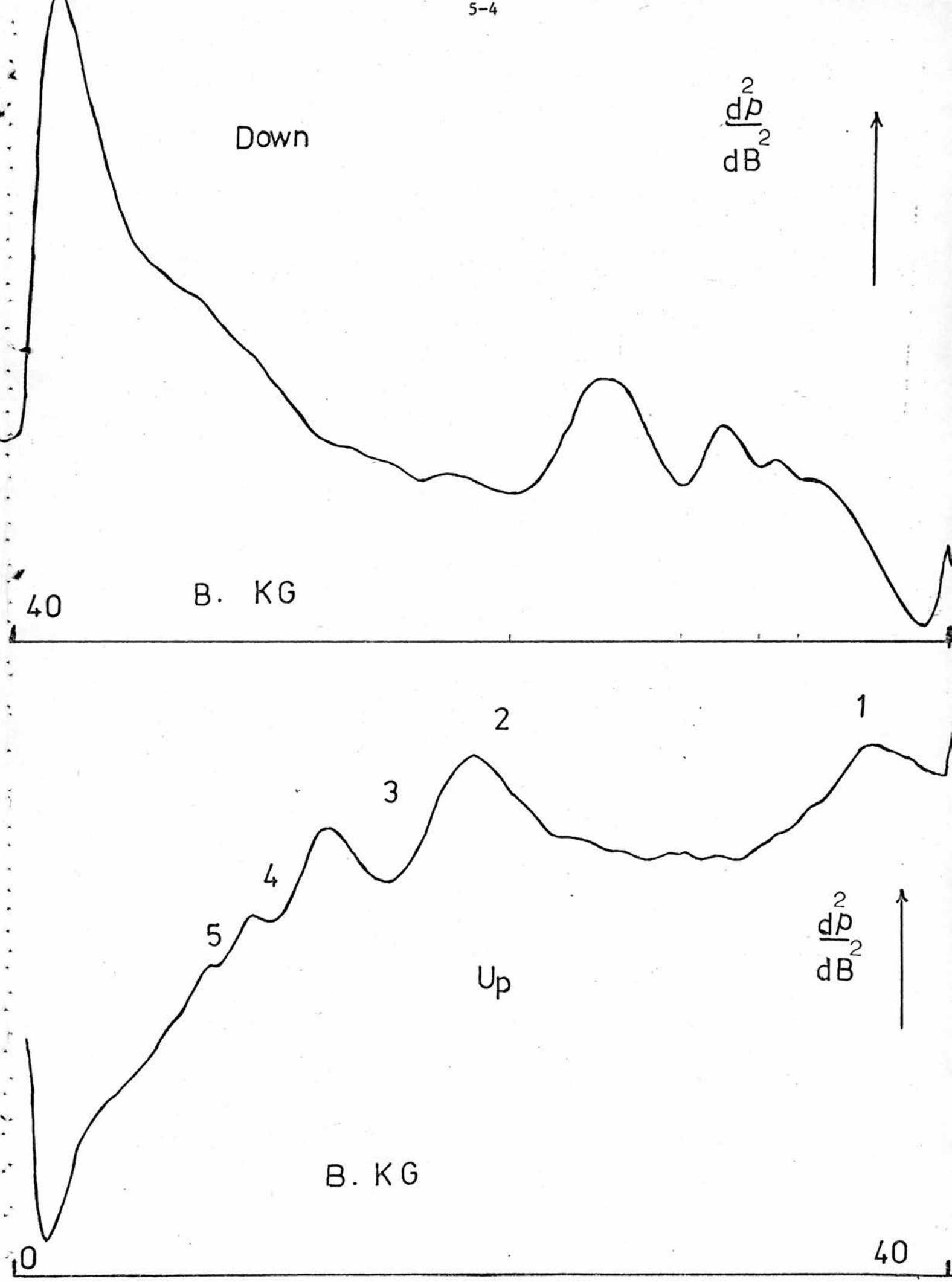


Fig. 5-3

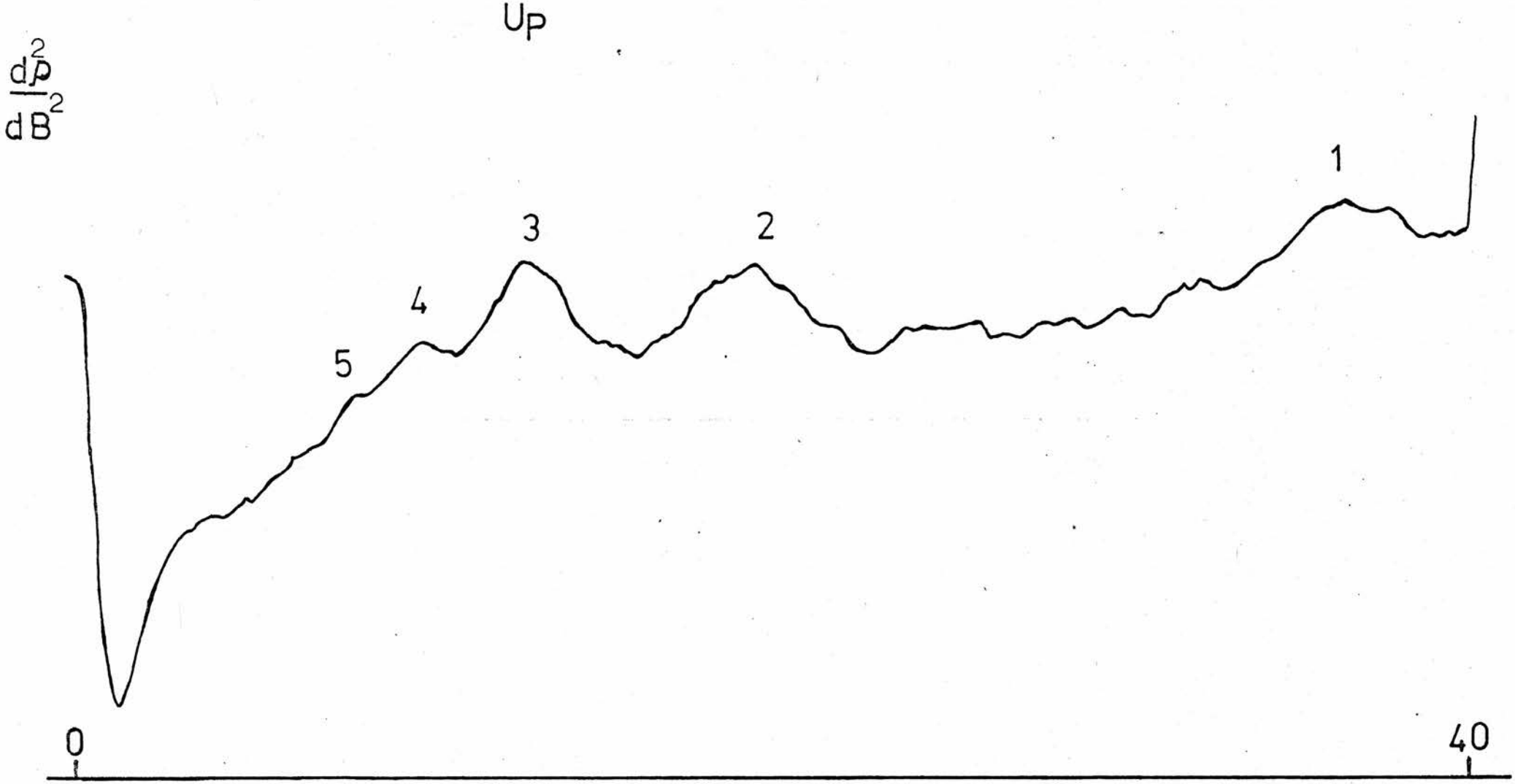


Fig. 5-4

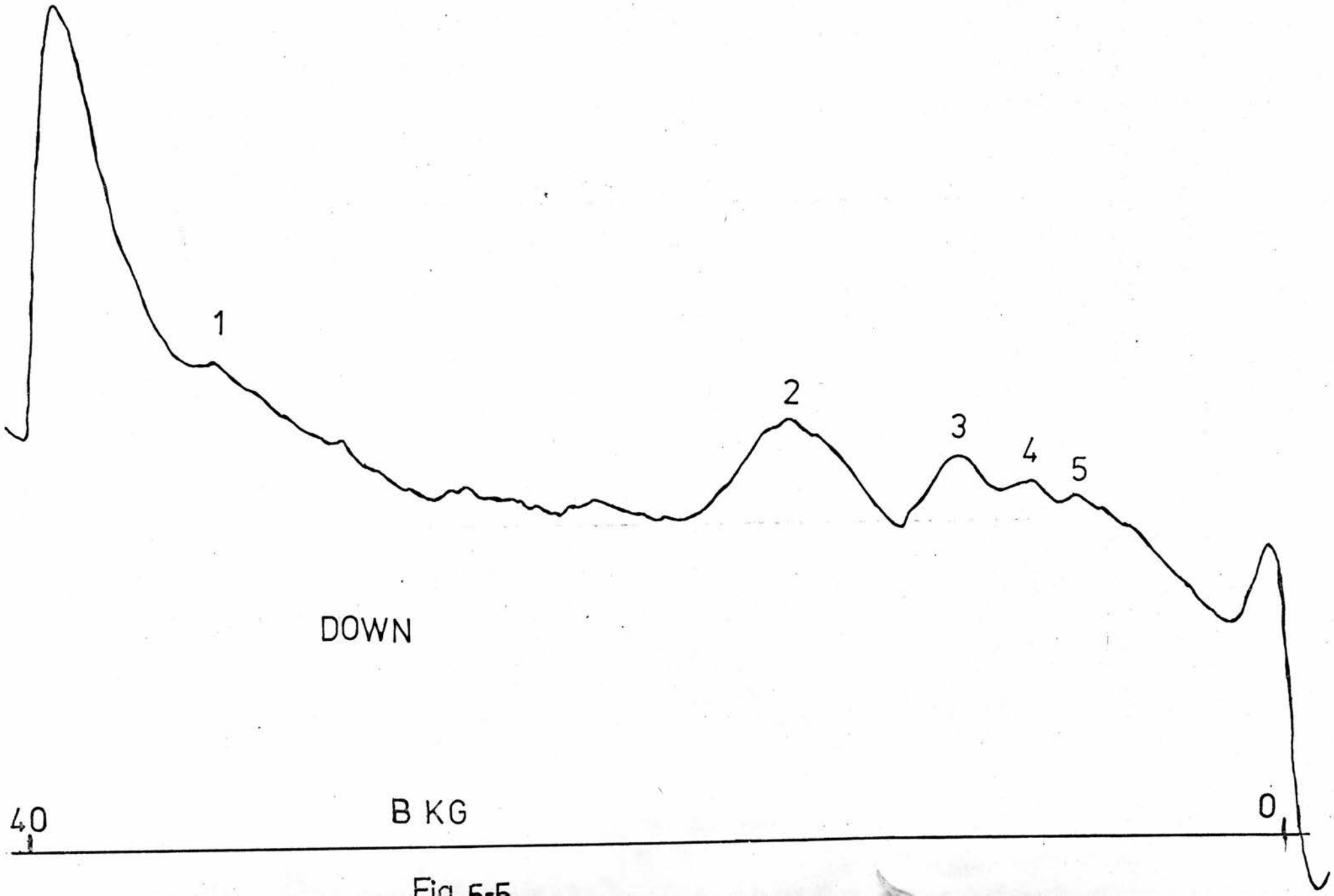


Fig 5-5

5.1.1 Amplified Differential Technique

For J in (100) direction and B in (010) direction, we measured the transverse magnetoresistance by the Digitally Recorded Technique Section 4.2.3, at 77°K. The maxima on the transverse magnetoresistance curve Fig [5-1] were located at B=34,17,11.3, and 8.5 Kgauss corresponding to N = 1,2,3, and 4 respectively. These coincide very well with what has been reported by Gurevich et al (1964) B = 34,17,11.0, and 6.5 Kgauss at 90°K, since the period and phase of oscillation in the transverse magnetoresistance do not depend on the temperature and carrier concentration [Gurevich et al 1964 and Parfenev et al 1974].

5.1.2 Direct Differential Technique

Then we employed for the same sample the Direct Differential Technique Section 4.2.2 and 4.3. We saw earlier on that this method gives $\frac{d^2\rho}{dB^2}$. We ensured that the two sections of the differentiator had approximately the same RC time constant, and removed the time delay by sweeping the magnetic field up and down.

The data of InSb derived from Fig (5-1), Fig (5-2), Fig (5-3), Fig (5-4) and Fig (5-5) are shown in Table (5-1) within the experimental error which arises for example from the GaAs thermometer (*which we find affects the field position by ± 0.36l%*) and the discontinuity of the sweep which unavoidably occurs at the beginning & end of the sweep and gives rise to an error of ∓ 3.1% at the beginning and end.

Table [5-1]

| N | $B_1$ Kgauss | $B_2$Kgauss | $B_5$ Kgauss | $B_d$ Kgauss |
|---|---|---|---|---|
| 1 | 32.5 | 35.1 | 35,0 | 34,0 |
| 2 | 17,4 | 16,9 | 17,5 | 17,0 |
| 3 | 11,4 | 11,4 | 11,4 | 11,3 |
| 4 | 8,4 | 8,6 | 8,8 | 8,5 |
| 5 | 6,7 | 6,7 | 7,1 | - |

In Table 5-1

$B_1$ - Fig (5-2) 1 min. sweep
$B_2$ - Fig (5-3) 2 min. sweep
$B_3$ - Fig (5-4) and Fig (5-5) 5 min sweep } Direct Differential Technique,

Bd - digitally recorded Technique.

Comparing with the data of other workers we have

| N | Bst.1 | Bst.2 | BG |
|---|---|---|---|
| 1 | 33.7 | 33.4 | 34.0 |
| 2 | 16.1 | 16.32 | 17.0 |
| 3 | 10.73 | 10.83 | 11.0 |
| 4 | - | 8.1 | 8.5 |
| 5 | - | 6.49 | 6.5 |

Bst.1 Stradling & Wood (1970) Differentiat T.
Bst.2 Stradling & Wood (1968) Concellation T
BG Gurevich et al (1964) Digitally Recorded Technique.

The data of Stradling & Wood (1970) and (1968) are corrected for the non parabolicity of the band.

The error arising in the Direct Differential Technique is mostly from the prominent artifact [*reported and named by Blakemore et al 1974*] at the beginning and end of the sweep due to the sweep unit. We add here that this prominent artifact arises from the RC network giving an error near t = o as discussed in section 4-3. It is due to the fact that the voltage across R is not negligible compared with that across C. This error is more pronounced for larger sweep time which means larger time constant RC.

5.2 PbS

We used for the investigation of the magnetophonon phenomena in n-type PbS three samples with carrier concentration and mobility given in Table (5-2). Four different Techniques for this study will be discussed below,

Table (5-2)

| Sample | Concentration ($cm^{-3}$) | Mobility ($cm^2\ v^{-1}\ sec^{-1}$) |
|---|---|---|
| I | $4.0 \times 10^{16}$ | 5163 |
| II | $4.8 \times 10^{16}$ | 5615 |
| III | $5.4 \times 10^{16}$ | 4045 |

For the sample of concentration $n = 5.4 \times 10^{22}\ m^{-3}$ we calculate

$$E_{Fo} = 10.2 \times 10^{-22}\ J,$$

and at 77°K.

KT is again $10.6 \times 10^{-22}$ J,

Since $E_{Fo}$ is slightly less than KT for this sample it is just non-degenerate and the other samples with smaller n are also nondegenerate.

From the above data we can calculate $\hbar\omega_c$

since

$$\omega_c = \frac{eB}{m^*} = \frac{\text{coul.} \times 10^3 \times 10^{-4}\ \text{Kgm}}{\text{Kgm.Sec.A}}$$

For B = 40 Kgauss

$$\omega_c = \frac{1.6 \times 10^{-19}\ \text{coul} \times 10^3 \times 40 \times 10^{-4}}{0.08 \times 9.108 \times 10^{-31}}$$

$$\omega_c = 88.0 \times 10^{11}\ sec^{-1}$$

and

$$\hbar\omega_c \sim 9.3 \times 10^{-22}\ J,$$

so

$$\hbar\omega_c \approx KT$$

This work was carried out at 77°K with the magnetic field applied in the (010) direction and a constant current of 10 ± .01 ma applied in the (100) direction. Because of the difficulty in observing the oscillations in PbS we also employed the following techniques.

5-2-1 Digitally Recorded Technique

The curve shown in Fig (5-6) was obtained by point by point measurement. As seen in the figure, oscillations are observed but are very small compared to those of InSb shown in Fig (5-1), being less than 2% of the monotonic part.

The error in locating the exact position of the maximum can exceed the GaAs thermometer error. This error due to the magnetic field was estimated by comparing the InSb data with and without the thermometer.

5-2-2 Direct Differential Technique

Fig(5-7)to (5-12)

Here we apply the direct differential technique to sample I, which, as we said earlier, displays the second derivative of the resistivity with respect to the magnetic field.

The time constant of the RC networks should be less than T (realtime) at the chosen sweep rate. Because we are sweeping the magnet current instead of the field some error will be introduced. The time delay cancellation is not perfect because the magnetophonon effect is periodic in $\frac{1}{B}$, not in B itself.

To detect these small oscillations in n-type Pbs we have to accept some distinction by allowing the time constant of the Differentiator to be nearly equal to T i.e. $RC \leqslant T$. This will increase the error and the noise, and also make the prominent artifact arising from the sweep and the differentiator more pronounced.

The maximum sweep rate is controlled by the design of the superconducting solenoid.

We hope that technical difficulties arising from the sweep time and differentiator can be mostly eliminated by taking the average value of graphs (5-7) to (5-12) for different RC, and sweep times.

The error due to the discontinuity at the initiation and end of the sweep which is unavoidable, has been measured and found to be $\pm$ 3.1% at the end and beginning of the sweep, and the error of the field position due to the thermometer (GaAs) which is $\pm$ 0.36% has been corrected as well. The values of the minimum of $\frac{d^2\rho}{dB^2}$ should occur at almost the same fields as the maximum of $\rho$ itself - Blakemore et al (1974) and Blakemore and Kennewell (1974), compare the relative merits of field sweep and field modulation methods for displaying $\frac{d^2\rho}{dB^2}$ as a function of field.

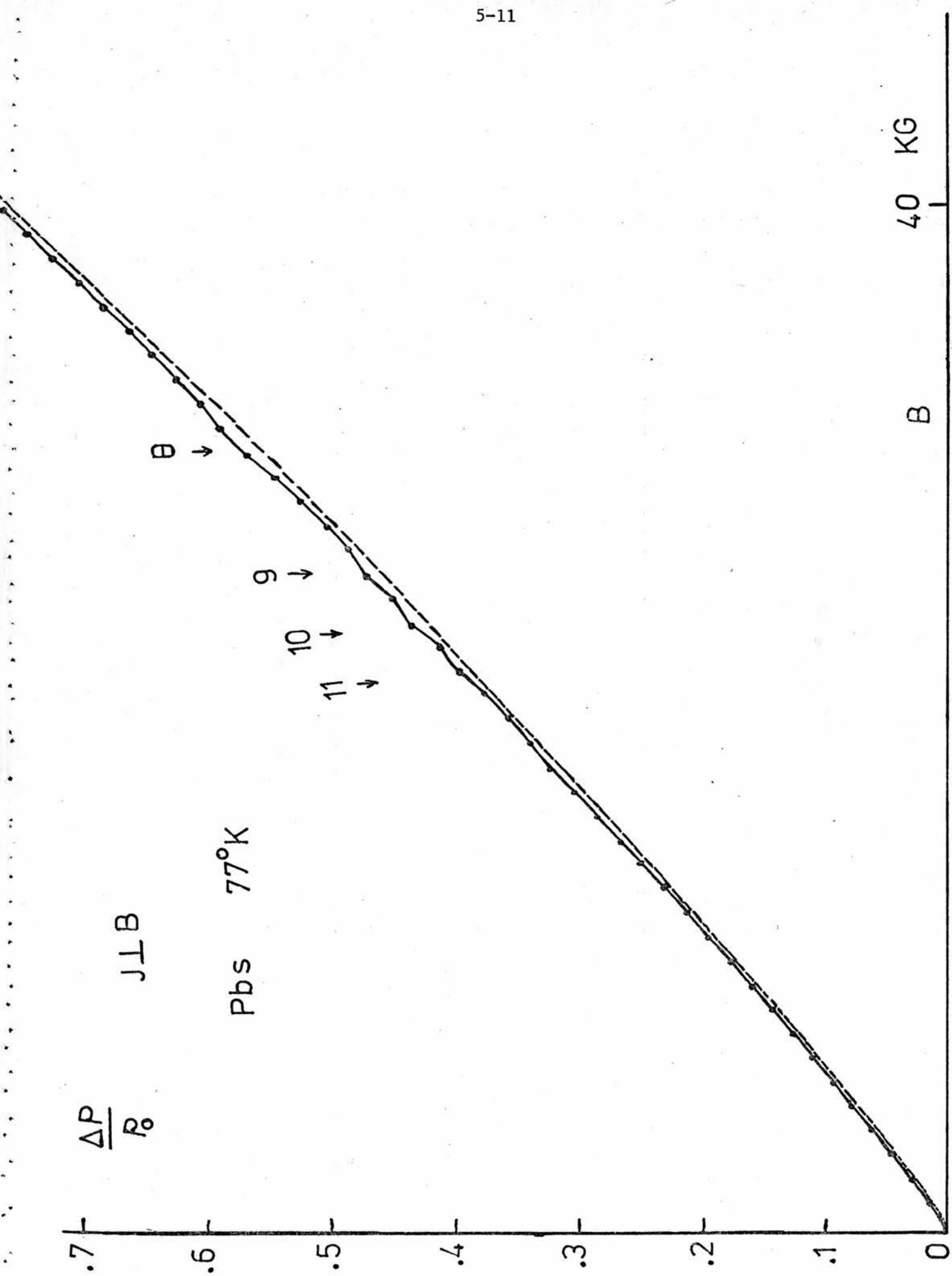


Fig. 5-6

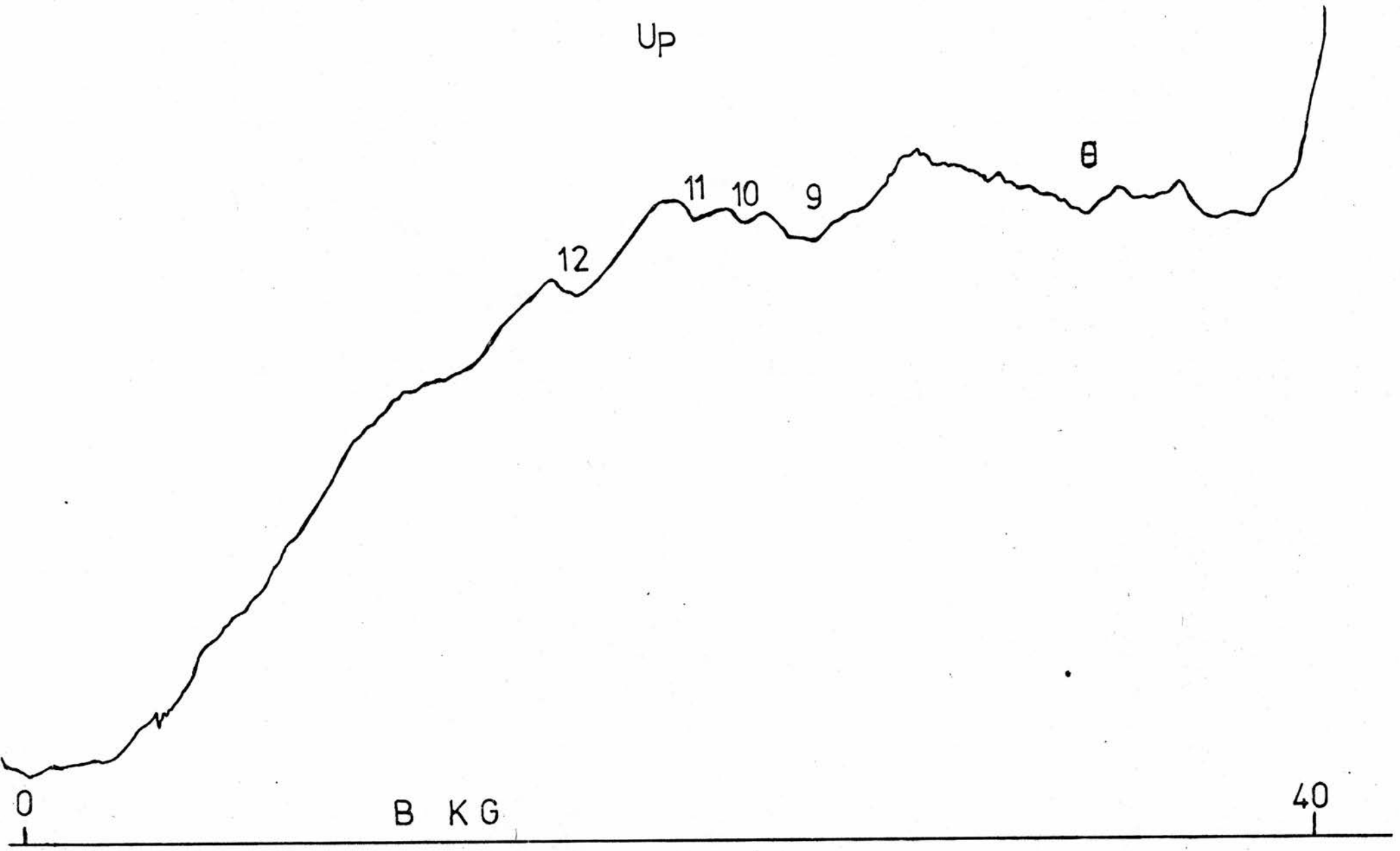


Fig. 5-7.A

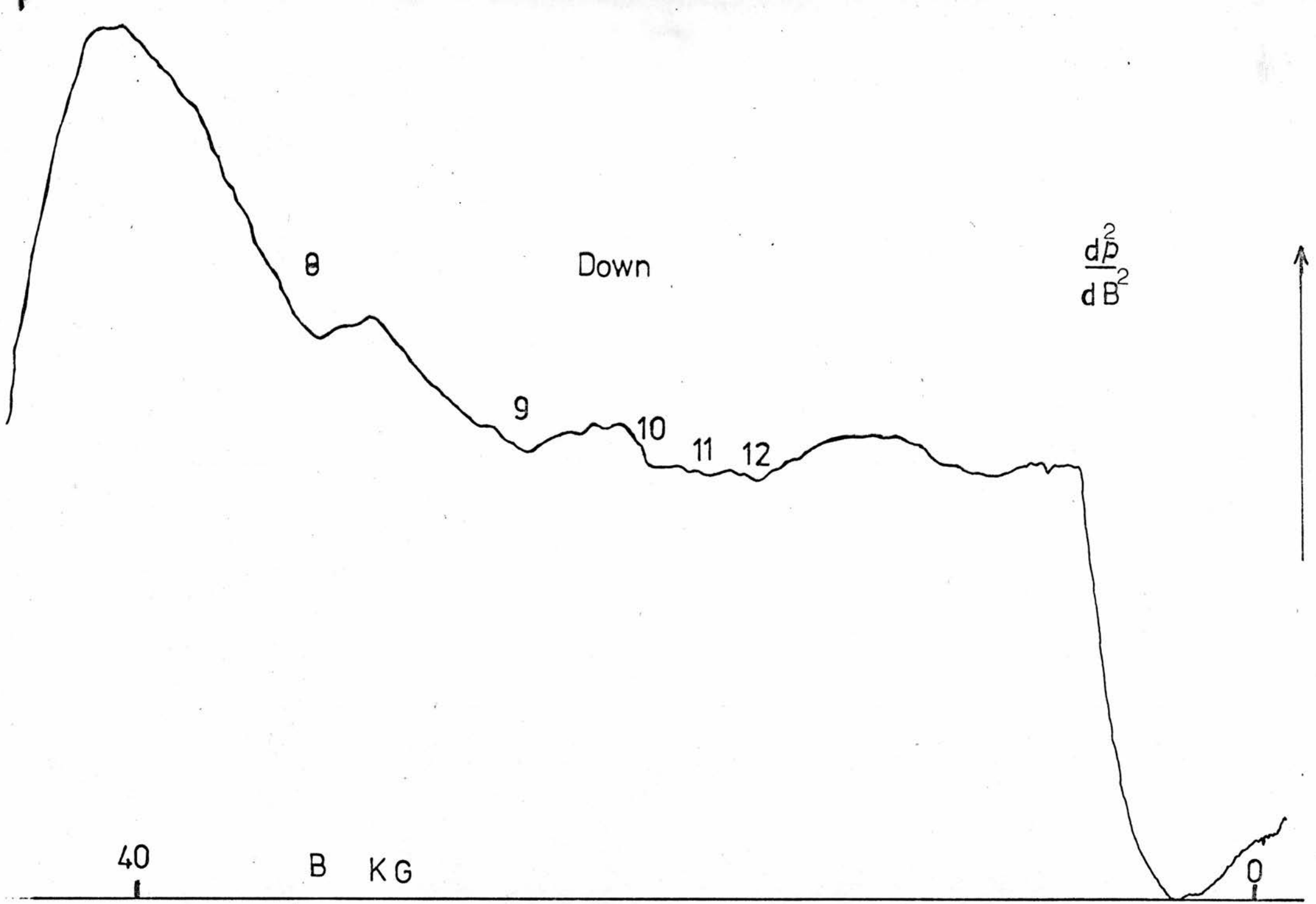


Fig.5-7 B

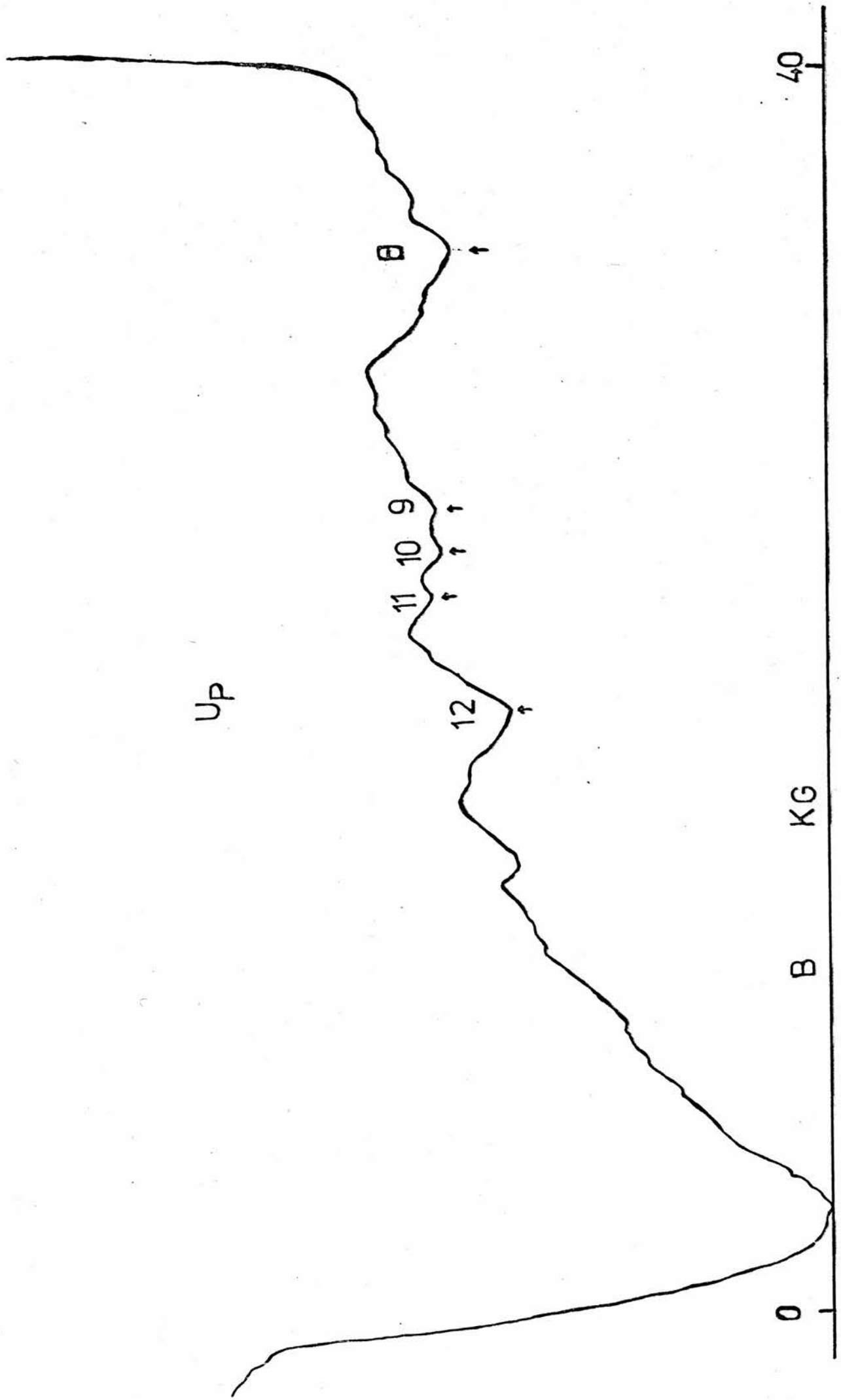


Fig.5-8.A

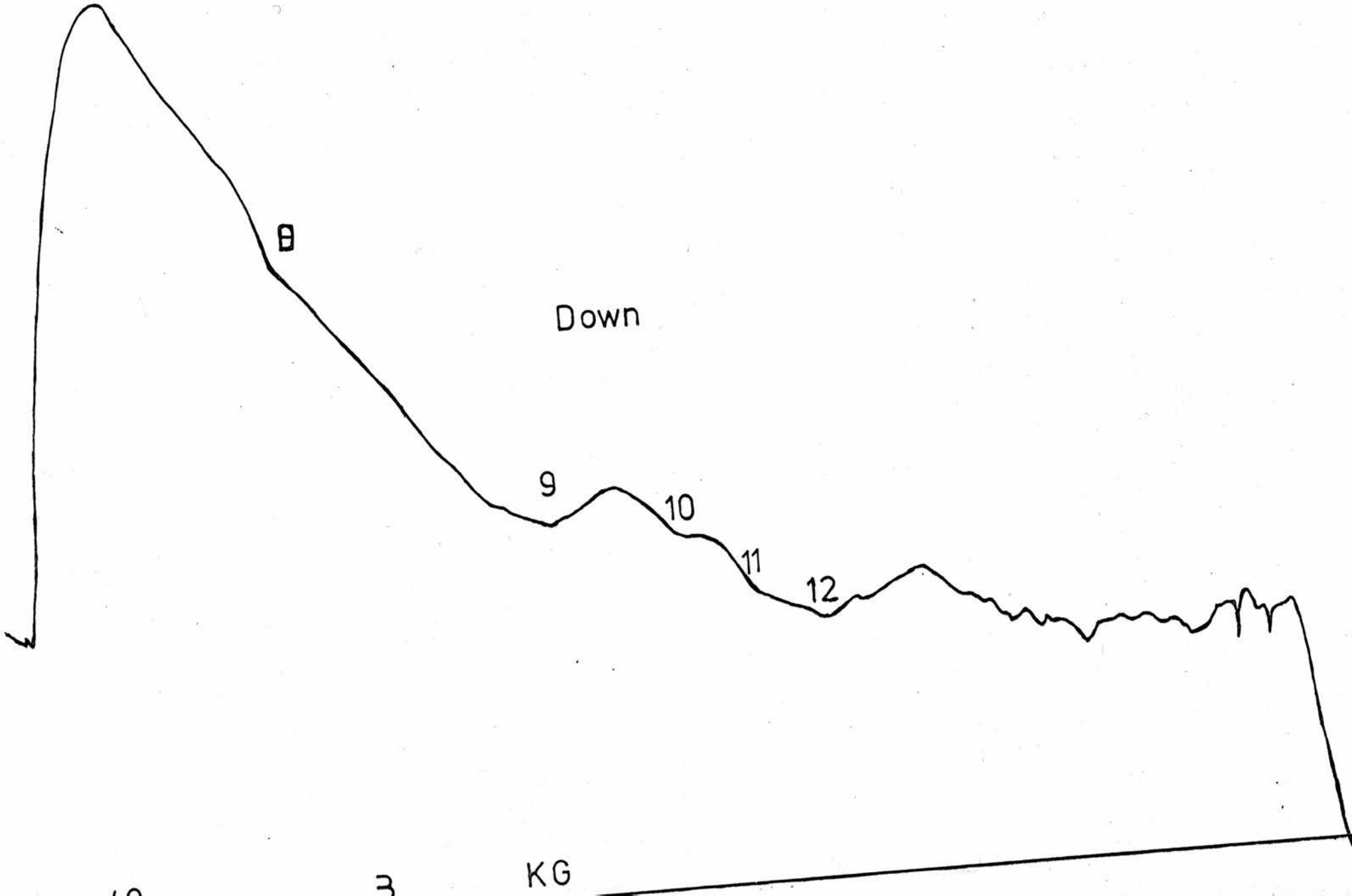
8
Down
9
10
11
12
KG
3

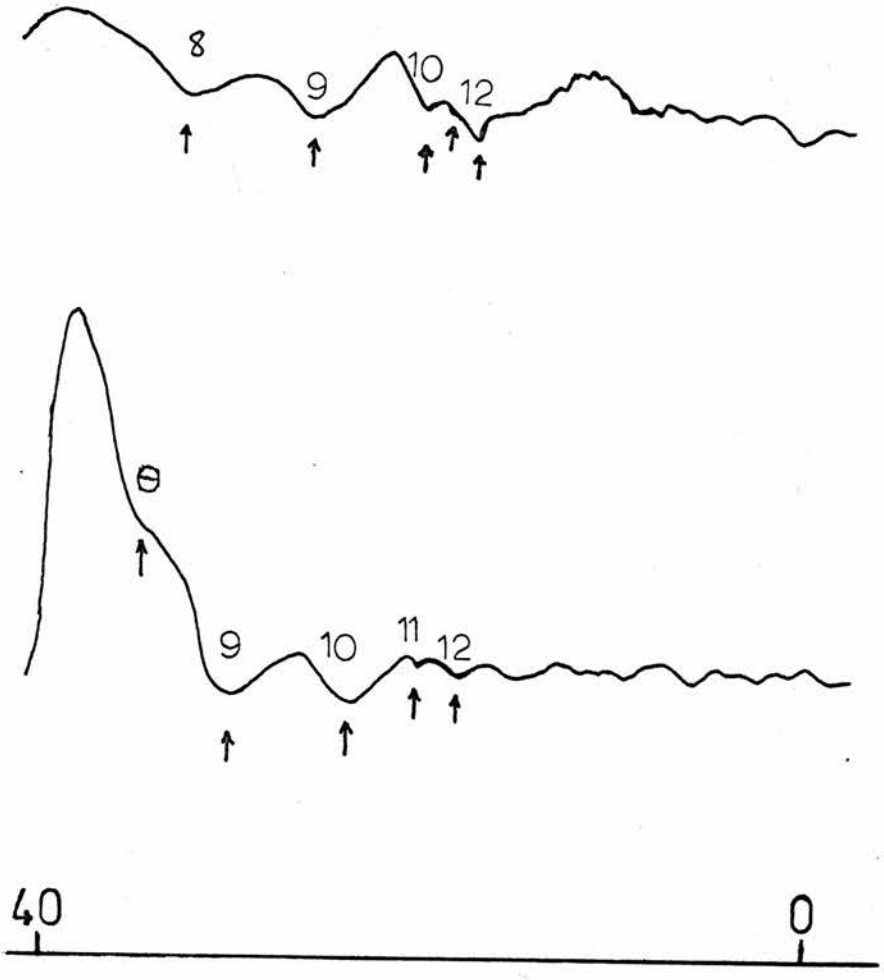


Fig. 5-9

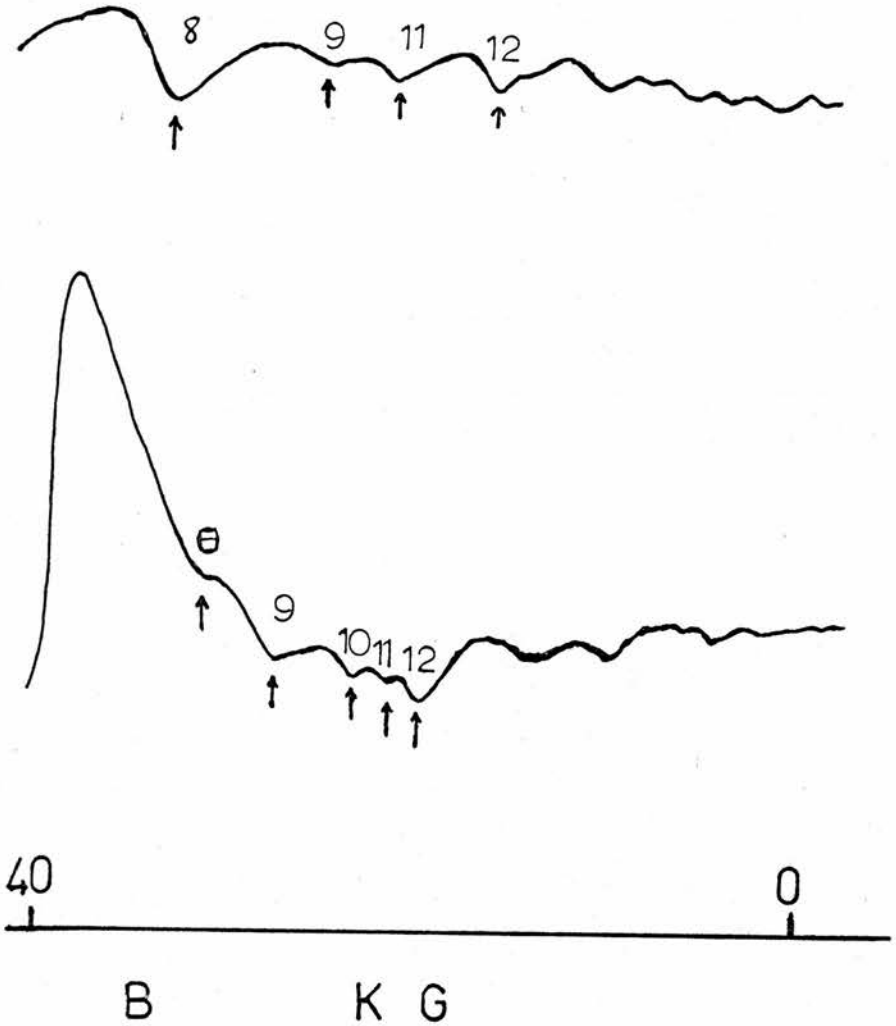


Fig. 5-10

Fig. 5-11

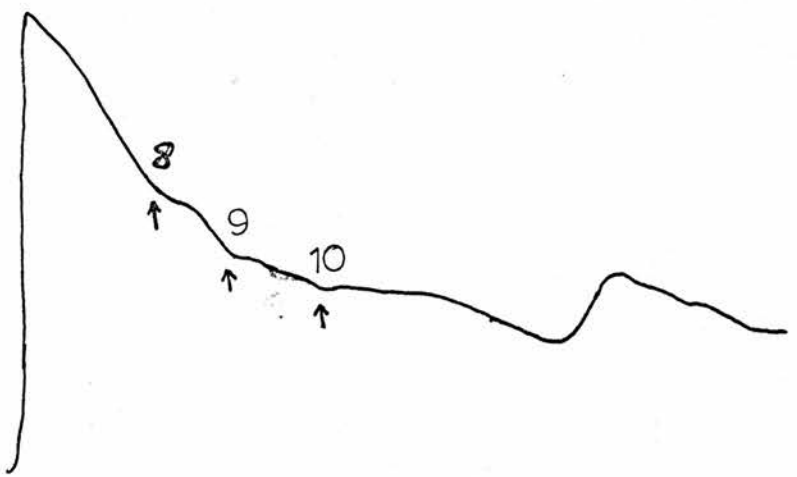


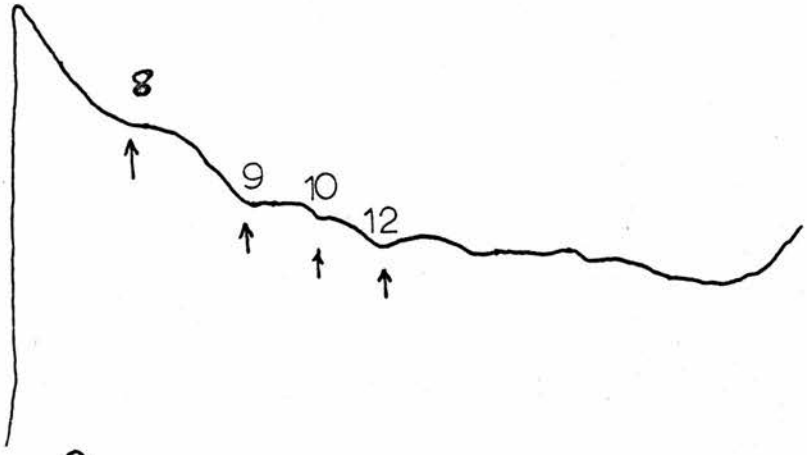


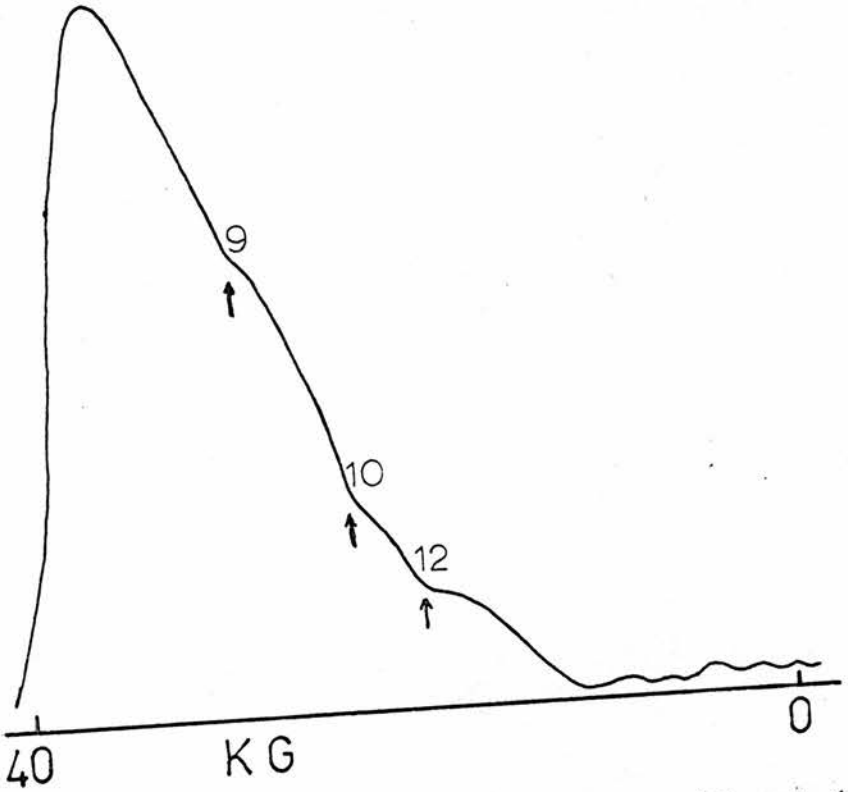


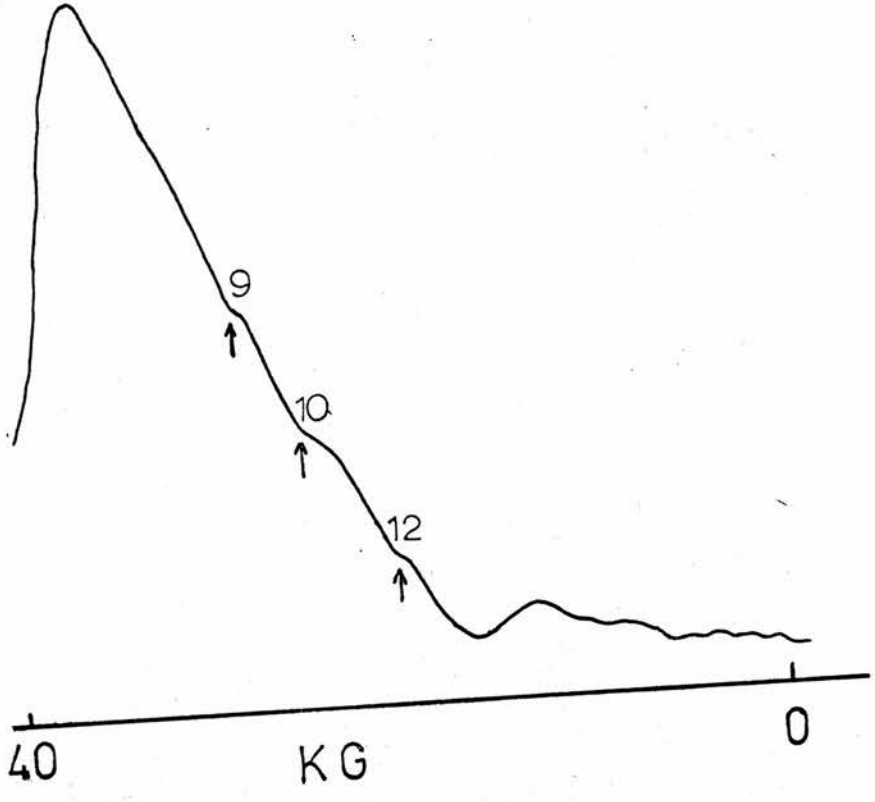


Fig.5-12

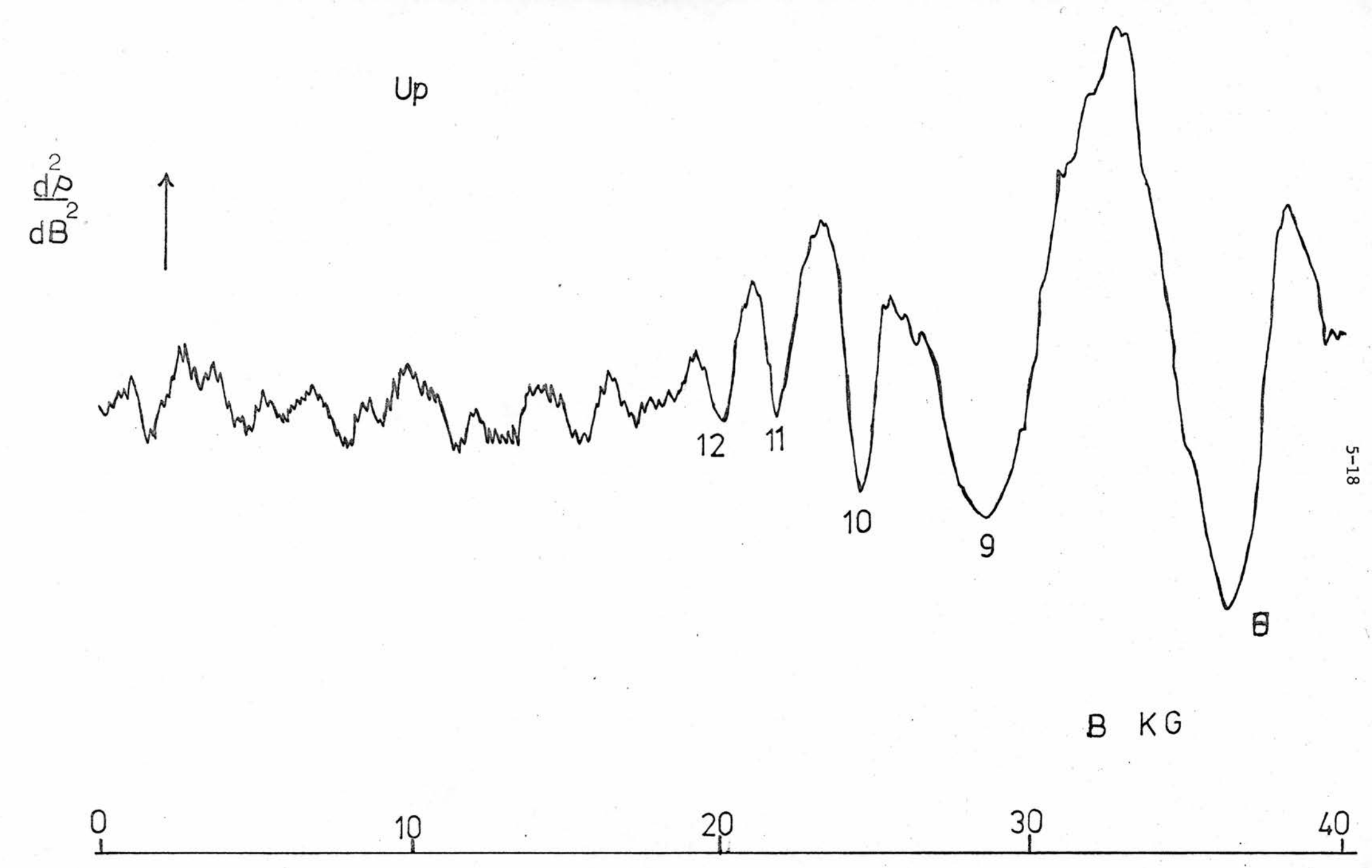


Fig. 5-13.A

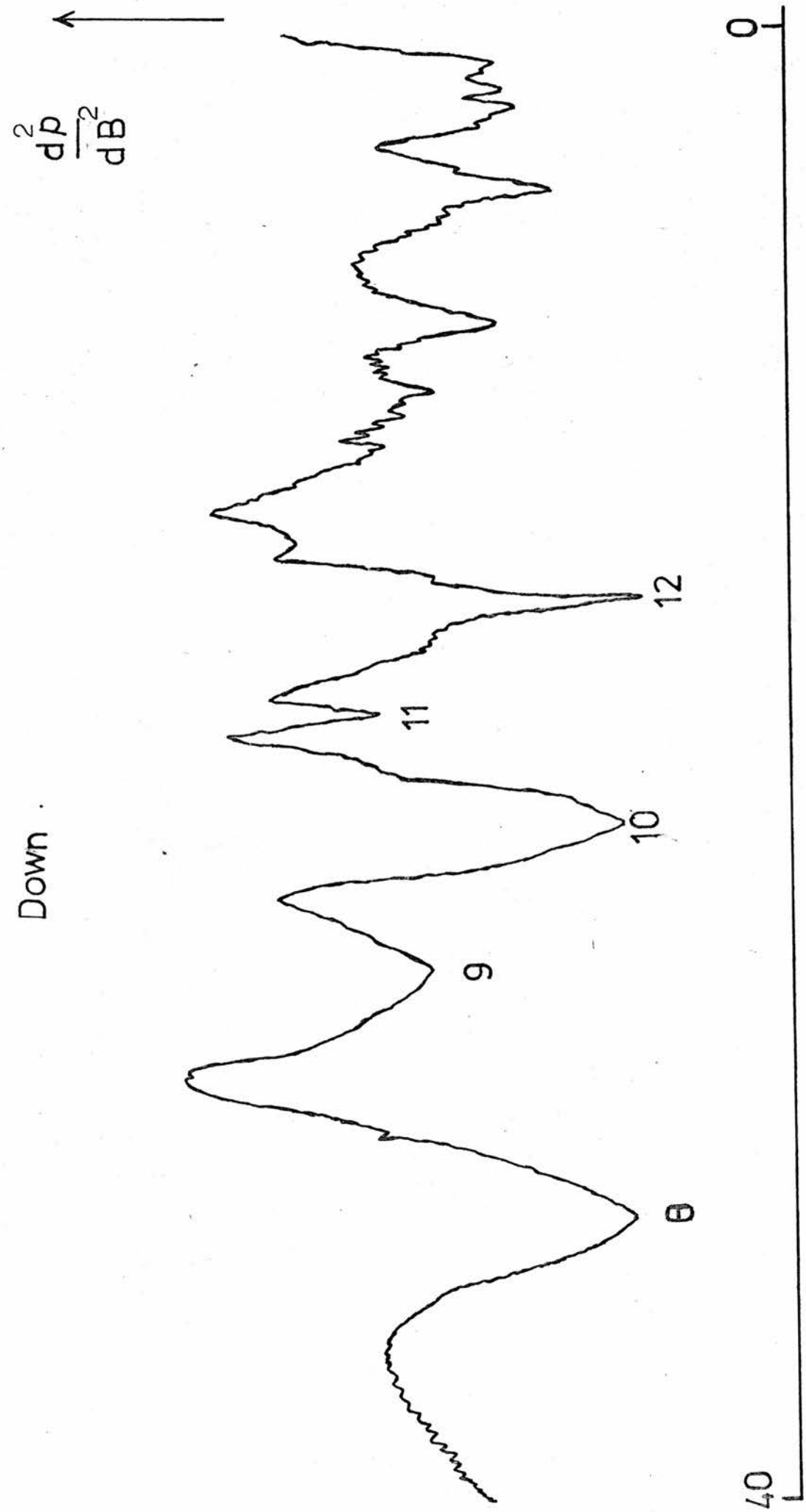


Fig. 5-13.B

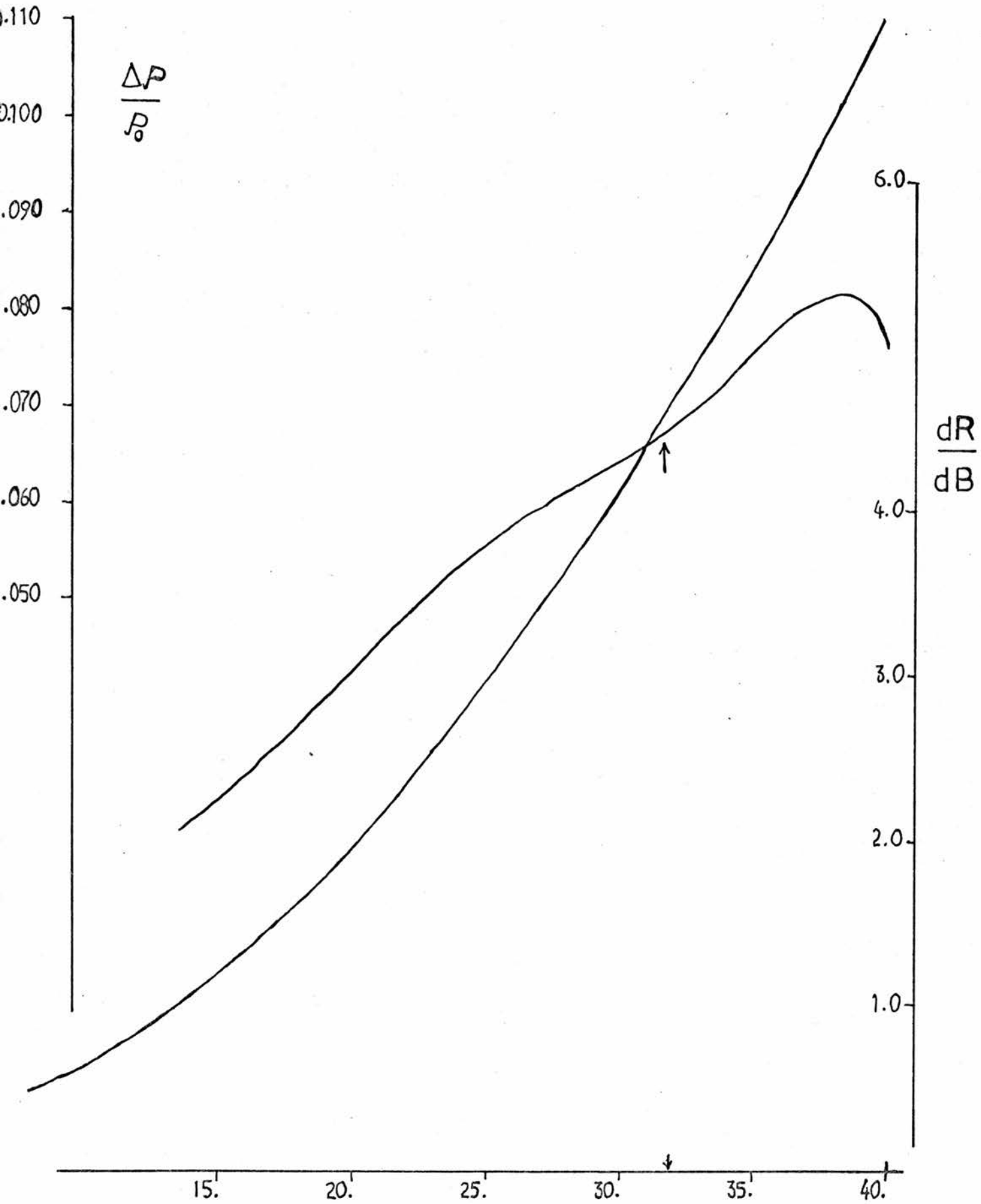
.110
.100
.090
.080
.070
.060
.050
ΔP/P0
6.0
4.0
3.0
2.0
1.0
dR/dB
15.
20.
25.
30.
35.
40.

Fig. 5-14

The values of the minimum of $\frac{d^2\rho}{dB^2}$ in Table (5-2) have been corrected accordingly.

5-2-3 Amplified Differential Technique

This is based on sweeping the field linearily with time while amplifying the sample voltage by a Keithley 149 milli-microvoltmeter, and differentiating by two RC networks. This technique gives $\frac{d^2\rho}{dB^2}$ and allows us to use small RC values i.e. $\frac{RC}{T}$ will be much less than 1,

This can get rid of error at the extrema due to high RC and also to get rid of the prominent artifact at the initiation and end of the field. However an increase in amplification gives an increased noise which is counteracted to some extent by the small bandwidth of the DC amplifier employed. Also the necessity of raising the amplification because of the small $\Delta\rho$ in PbS tends to overload the recorder amplifier.

We found that Fig (5-13) A, B is the best we can get for the sample II PbS n-type. The average values of the minimum for sweeping the field up and down are listed in Table (5-2).

There is no thermometer correction here because we used a different thermometer, and the discontinuity of the sweep was minimized by using an X-Y recorder and much smaller RC.

5-2-4 Computerized Technique

For sample III which has the lowest mobility we found neither of the above techniques very good, so we used this technique discussed in Section (4.2.4).

We have been able by this technique to analyse one minima in this sample Fig. (5-14) , which is listed in table (5-2). This gives $\frac{dR}{dB}$ where $R = \frac{\Delta\rho}{\rho_o}$ .

Table (5-2)

| N | sample I | | sample II | sample III |
|---|---|---|---|---|
| | B max of $\frac{\Delta\rho}{\rho_o}$ KG | B min of $\frac{d^2\rho}{dB^2}$ KG | B min of $\frac{d^2\rho}{dB^2}$ | B min of $\frac{dR}{dB}$ KG |
| 8 | 30.57 | 32.3 | 33.1 | 31.8 |
| 9 | 25.7 | 26.4 | 26.1 | - |
| 10 | 23.3 | 22.9 | 22.9 | - |
| 11 | 21.4 | 20.8 | 20.2 | - |
| 12 | - | 18.2 | 17.9 | - |
| | A | B | C | D |
| Fig | 5-6 | 5-7 to 5-12 | 5-13 A & B | 5-14 |

As follows from the early theoretical and experimental research in magnetophonon effect, the position of the extrema of the transverse magnetoresistance, and the period of the magnetophonon oscillation should not depend on the electron concentration.

We can see the above differences arise from different instrumentation and the proper average value of these is the required one.

From Table (5-2) we can see that the minima of N=9, and 10 are less distorted than the others at the initiation and end of the field, and the experimental error due to different techniques are more pronounced at the end and initiation of the field.

So in taking a graphical, arithmetic average we must not forget these facts.

5-2-5 Average of the experimental data

To obtain good averaged values from the four different techniques employed we have divided the data into two parts:- a) in which the maxima of $\frac{\Delta\rho}{\rho_o}$ have been taken, digitally recorded data, and which includes the $\frac{dR}{dB}$ value of sample III, and b) in which the minima of $\frac{d^2\rho}{dB^2}$ have been taken, differential data.

The quantity NB = $\frac{\omega_{LO} m^*}{e}$ is a useful parameter. In table (5-3) the average NB values are compared with the experimental values and the calculated error given for each method.

Table (5-3)

| $N = \frac{B_o}{B}$ | NB average defined as $= \frac{\omega_{LO} m^*}{e}$ K gauss | B average K gauss | % experimental error in NB of digitally recorded data A,D in table (5.2) | % experimental error in NB of differential data B,C in table (5-2) |
|---|---|---|---|---|
| 8 | 232.2 | 29.03 | +6.5 | +11.9 |
| 9 | 234.27 | 26.03 | -1.23 | + 0.95 |
| 10 | 234.24 | 23.4 | -0.41 | - 2.1 |
| 11 | 234.01 | 21.3 | +0.59 | - 5.04 |
| 12 | 233.02 | 19.42 | ~ | - 7.36 |

5-2-6 Experimental phase shift correction

Apart from above experimental sources of possible error, any maximum of $\rho$ or minimum of $\frac{d^2\rho}{dB^2}$ is phase shifted from the magnetic field at which the Landau level separation $\hbar\omega_c = \frac{\hbar eB}{m^*}$ is an exact sub-multiple of the long wave LO phonon energy $\hbar\omega_{LO}$, as a consequence of the field dependence of the oscillatory amplitude [Blakemore and Kennewell 1974]. This topic has been mentioned and corrected for by a number of authors for example Stradling and Wood (1968), Wood (1970), Harper et al (1973), Firsov et al (1964) and Shalyt et al (1964). The phase shift is attributed to the considerable deviation from parabolicity of the conduction band. This phase shift which arises from the variation in amplitude of the resonance peaks [*according to Blakemore & Kennwell 1974*] has been examined as a feature of both differentiated and un-differentiated recording of the oscillations. They found that it is greater in the former case.

From the presented tables and formula which quote this shift we found that the following power law formula give the best fit to our data,

Case 1: For the digitally recorded data i.e, measurement of maxima of resistivity [A in table (5-2)] , these maxima are given by the field for which

$$\left(\frac{2\pi B_o}{B}\right) \tan \left(\frac{2\pi B_o}{B}\right) = -P \qquad [5\text{-}1]$$

Case 2: For the differentiated date where $\frac{d^2\rho}{dB^2}$ has been measured, the minima of the second derivative occur for the series of fields which are solutions of

$$\tan \left(\frac{2\pi B_o}{B}\right) = \left(\frac{2-P}{2\pi B_o/B}\right) \left(\frac{3(2\pi B_o/B)^2 - P(P-1)}{(2\pi B_o/B)^2 - 3(P-1)(P-2)}\right) \qquad [5\text{-}2]$$

for equation (5-1) and (5-2)

$$N = \frac{B_o}{B}$$

and P is a necessary integer.

The most convenient way of solving these equations is graphically.

For our case we find P = 6 for n-type PbS give a reasonable fit for both cases. In table (5-4) we tabulate the corrected NB values according to equation (5-1) and (5-2).

Table (5-4)

| $N = \frac{B_o}{B}$ | NB corrected phase shift KG | B corrected KG | % experimental phase shift in NB of digitally recorded data | % experimental phase shift in NB of differential data |
|---|---|---|---|---|
| 8 | 233.88 | 29.23 | +6.60 | +12.2 |
| 9 | 234.71 | 26.08 | -1.4 | + 0.8 |
| 10 | 234.73 | 23.5 | -0.6 | - 2.27 |
| 11 | 234.76 | 21.34 | -0.4 | - 5.2 |
| 12 | 234.73 | 19.56 | ~ | - 7.5 |

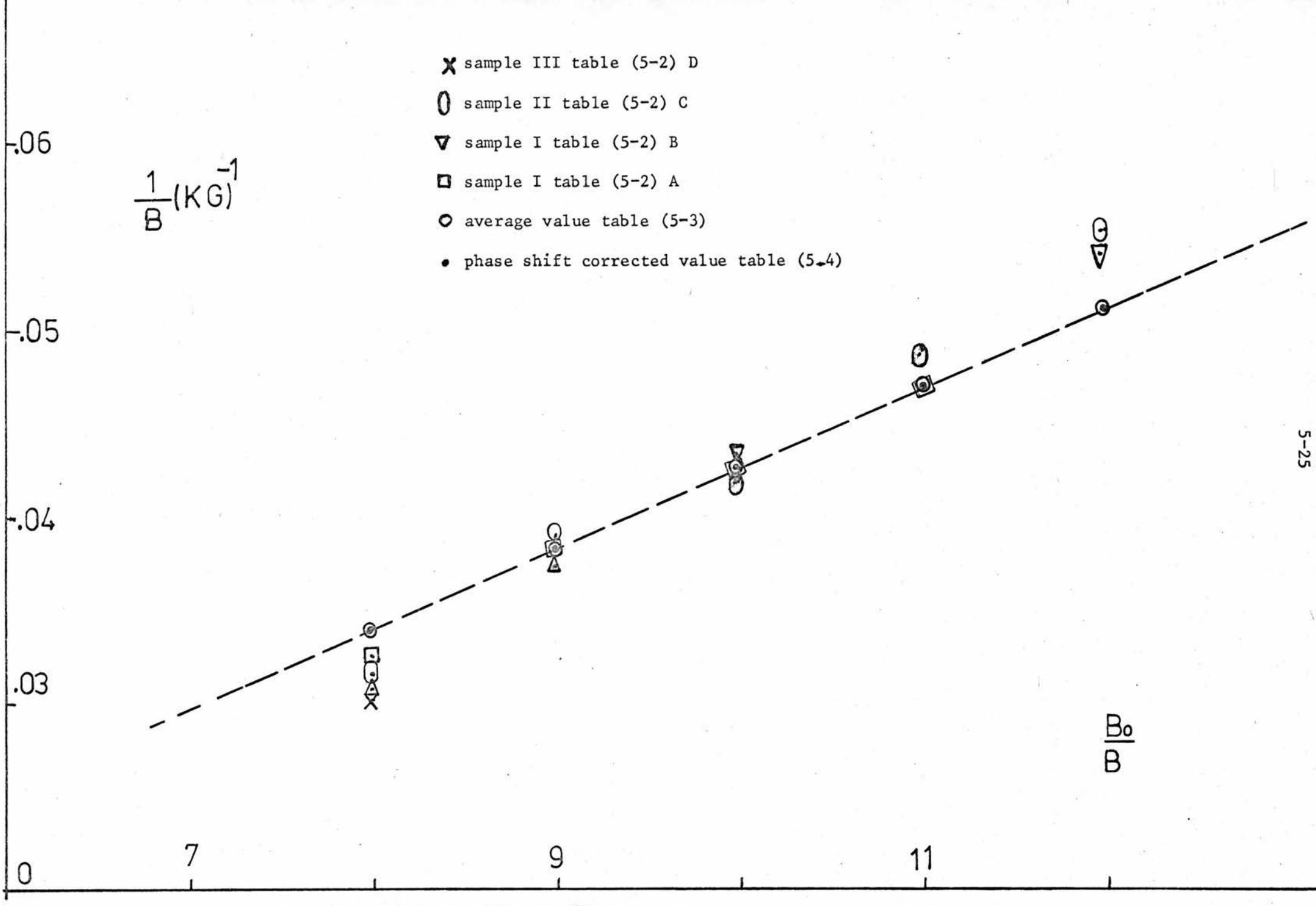
sample III table (5-2) D
sample II table (5-2) C
sample I table (5-2) B
sample I table (5-2) A
average value table (5-3)
phase shift corrected value table (5-4)
$\frac{1}{B}(KG)^{-1}$
.06
.05
.04
.03
0
7
9
11
$\frac{B_0}{B}$

Fig. 5-15

## 5-2-7 Band edge effective mass calculation

As we said earlier

$$B_o = \frac{\omega_{LO}\, m^*}{e}$$ where $B_o$ is the field of N=1,

And because $$N = \frac{B_o}{B}$$

So $$NB = \frac{\omega_{LO}\, m^*}{e}$$

If the fields at which the extrema occurred were multiplied by the appropriate integer, the same field was obtained for all values of N as would be expected if the above equation was rigorously obeyed

then $$m^* = \frac{eNB}{\omega_{LO}}$$

and $$\frac{m^*}{m} = \frac{eNB}{\omega_{LO}\, m}$$

$e = 1.602 \times 10^{-19}$ coul.

$\omega_{LO} = 44.8 \times 10^{12}$ sec $^{-1}$ from table [3-1]

at 296$^{o}$K in L point of Brillouin zone

$m = 9.108 \times 10^{-31}$ Kgm

$NB = 234.6$ [average from table [5-4]] Kgaus

So

$$\frac{m^*}{m} = \frac{1.6 \times 10^{-19} \text{ coul} \times 234.6 \times 10^{3} \times 10^{-4} \text{ Kgm/S}^2\text{,A}}{44.8 \times 10^{12} \times 9.1 \times 10^{-31} \text{ sec}^{-1} \text{ Kgm}}$$

and $$\frac{m^*}{m} = 0{,}092 \pm 0{,}002$$

which coincides with a period $\Delta(\frac{1}{B})$ from graph (5-15)

of $$\Delta(\frac{1}{B}) = 4{,}26 \times 10^{-3} \quad (KG)^{-1}.$$

## 5.2.8 Polaron Correction

The polaron contribution is discussed in chapter II. If we use Palmer's (1971) equation we can get the cyclotron effective mass which is equal to

$$m^*_{cycl} = m^*_{MP}/(1 + \eta \frac{\alpha}{3})$$

for our case:

$m^*_{MP} = 0.092\ m_o$

$\alpha = 0.33$ for PbS at $77^oK$ Dalven (1971)

$\eta = 0.73$ numerical factor (Palmer 1971)

so

$$m^*_{cycl} = 0.092/(1 + 0.73 \frac{0.33}{3})$$

$m^*_{cycl} = 0.085\ m_o$ cyclotron effective mass or low-frequency mass.

To obtain the high frequency or "bare" mass we use the following equation [*chapter II*] with Palmer (1971) numerical factor $\eta = 0.73$

$$m^*_{MP} = m^*_{bare}\ (1 + 0.73 \frac{\alpha}{2})$$

we get for

$$m^*_{bare} = 0.082\ m_o$$

which is the high frequency or bare mass.

## 5.2.9 Discussion of the Result

The band edge effective mass for n-type PbS was estimated from the results given in Fig. [5-15] and Table (5-4) and after applying experimental phase shift and polaron correction

| | Low-frequency mass | High-frequency mass |
|---|---|---|
| At $77^oK$ | $0.085\ m_o$ | $0.082\ m_o$ |

The accuracy in determining the mass is governed by the accuracy in determining the period of oscillation $\Delta(\frac{1}{B})$ and the accuracy in determining $\omega_{LO}$ which is reported to be within 3%.

The error of determining $\Delta(\frac{1}{B})$ does not exceed 2%.

In the absence of a more complete theoretical treatment of the magnetophonon effect, the systematic error involved in the various corrections cannot be estimated and could exceed the error in the determination of the experimental parameters.

However, the final mass values agree well with the following values determined by other techniques which are listed below:-

| Author | Technique | $m^*/m$ at $4.2^oK$ | $m^*/m$ at $77^oK$ |
|---|---|---|---|
| Cuff et al 1964 | de Haas-Shubnikov | 0.08±.01 | 0.0859±.01 (a) |
| Bernick & Kleinman 1970 | EPM calculation | 0.077 | 0.0832 (a) |

Other measurements and calculations of the effective mass of PbS are listed below.

| Author | Technique | $m^*/m$ |
|---|---|---|
| Finlayson & Greig (1958) | thermoelectric measurement | 0.11 b. |
| Palik et al (1964) | magneto-optical " | 0.11±.01 c. |
| Cuff et al (1964) | de Haas-Shubnikov | 0.08±.01 d. |
| Rabbi (1968) | APW calculation | 0.138 e. |
| Bernick & Kleinman (1970) | EPM calculation | 0.0774 f. |
| Ravich et al (1971) | ——— | 0.090 g. |

a. calculated by author from previous column

b. average at $77^oK$

c. at $77^oK$

d. at $4.2^oK$

e. at $4.2^oK$

f. at $4.2^oK$

g. density of state at $77^oK$

## Conclusion

We have observed magnetophonon resonances in n-PbS at 77K. The experiment was performed under non-degenerate conditions $E_{Fo} < kT$ and confirms the Gurevich and Firsov prediction.

The magnetophonon oscillations were observed in the transverse magnetoresistance of n-PbS single crystals whose electron concentration was around $5 \times 10^{16}$ $cm^{-3}$ determined from Hall measurements and whose mobility was in the region of $5 \times 10^{3}$ $cm^{2}$ $v^{-1}$ $sec^{-1}$ at $77^{o}K$.

Four different techniques were used to overcome the difficulties of seeing these small oscillations in PbS.

The minima of the $\frac{d^2\rho}{dB^2}$ and the maxima of $\frac{\Delta\rho}{\rho_o}$ were averaged and a phase shift correction, which arises from the variation in amplitude of the resonance peaks, was applied to them.

For these non-degenerate samples of PbS the non-parabolicity of the conduction band should be very small over the range of energy of interest as the longitudinal optical phonon energy of 0.029 eV is much less than the band gap of 0.307 eV. The increase in mass arising from the non-parabolicity should be small.

For these samples the free carrier screening is negligible because they are non-degenerate polar semiconductors. The minima of the magnetoresistance oscillation given in table (5-4), which occur at B = 29.2, 26.1, 23.5, 21.3, and 19.5 K gauss after correcting for phase shift are the N = 8, 9, 10, 11, and 12 resonances.

The period of the oscillation deduced from Fig. (5-15) is

$$\Delta\left(\frac{1}{B}\right) = 4.26 \times 10^{-3} \quad (KG)^{-1}$$

After a polaron correction has been applied to the magnetophonon effective mass we deduce a band-edge effective mass of 0.085 in low frequency approximation and 0.082 in high frequency approximation.

References


Adams, E.N. and Holstein, T.D., J. Phys. Chem. Sol. 10, 254 (1959).

Allgaier, R.S. and Scanlon, W.W., Phys. Rev. 111, 1029 (1958).

Allgaier, R.S., Phys. Rev. 112, 828 (1958); Proc. Int. Conf. Semicond. Phys. 1960 p.1037 (1961).

Argyres, P. and Roth, L., J. Phys. Chem. Sol. 12, 89 (1959).

Barker, J.R., J. Phys. C: Solid State Phys. vol. 5, 1657 (1972).

Bernick, R.L. and Kleinman, L., Solid State Commun. 8, 569 (1970).

Blakemore, J.S., Solid State Phys. London, Saunders & Co. (1970).

Blakemore, J.S. and Kennwell, J.A., J. Phys. C: Solid State Phys. vol. 8, 647 (1975).

Blakemore, J.S. et al, J. Phys. E: Sci. Instrum. vol. 8, 227 (1975).

Blatt, F.J., Physics of Electronic Conduction in Solids, McGraw-Hill (1968).

Conwell, E.M. and Weisskopf, V.F., Phys. Rev. 77, 388 (1950).

Cuff, K.F. et al, Proc. Int. Conf. Phys. Semicond. 7th 1964, p.677 (1964).

Dalven, R., Phys. Rev. B3, 1953 (1971).

Dalven, R., Solid State Phys. vol. 28, 179 (1973).

Davydov, B. and Shushkevitch, I., J. Phys. (U.S.S.R.) 3, 359 (1940).

Dingle, R.B., Proc. Roy. Soc. A211, 517 (1952).

Dworin, L., Phys. Rev. 140, A1689 (1965).

Eaves, L. and Stradling, R.A., J. Phys. C: 4, L42 (1971).

Eaves, L. et al, J. Phys. C: Solid State Phys. vol. 8, 1034 (1975).

Eaves, L. and Stradling, R.A., J. Phys. C5 L19 (1972).

Efros, A.L., Sov. Phys. Solid State 3, 9, 2079 (1962).

Ehrenreich, H., J. Phys. Chem. Sol. 8, 130 (1959).

Elcombe, M.M., Proc. Roy. Soc. Ser. A300, 210 (1967).

Elliott, R.J. and Gibson, A.F., An introduction to solid state physics and its applications, London (1974).

Finlayson, D.M. and Yau, K.L., Phys. Stat. Sol (a) 19, K79 (1973).

Finlayson, D.M. and Greig, D., Proc. Phys. Soc. 1, 49 (1958).

Finlayson, D.M. and Greig, D., Proc. Phys. Soc. 69, 796 (1956).

Finlayson, D.M. and Stewart, A.D., Brit. J. Appl. Phys. 17, 737 (1966).

Firsov, Y.A., Gurevich, V.L., Parfenev, R.V. and Shalyt, S.S., Phys. Rev. Lett. 12, 660 (1964).

Firsov, Y.A. and Gurevich, V.L., Sov. Phys. JETP, 14, 1, 367 (1962).

Fröhlich, H. and Mott, N.F., Proc. Roy. Soc. A171, 496 (1939).

Fröhlich, H., Polarons and Excitons, N.Y. Plenum Press (1963).

Gurevich, V.L. and Firsov, Y.A., Sov. Phys. JETP, 13, 1, 137 (1961).

Gurevich, V.L., Firsov, Y.A., Efros, A.L., Sov. Phys. Solid State, 4, 7, 1331 (1963).

Gurevich, V.L. et al, Physics of Semiconductors, Proc. 7th Int. Conf. (Paris) 1964 p.653 (1964).

Hall, R.N. and Racette, J.H., J. Appl. Phys. 32, Suppl. 2078 (1961).

Harper, P.G., Hodby, J.W. and Stradling, R.A., Rep. Prog. Phys. 36, 1, (1973).

Herman, F. et al, J. Phys. (Paris) 29, C4, 62 (1968).

Howarth, D.J. and Sondheimer, E.H., Proc. Roy. Soc. A219, 53 (1953).

Kaidanov, V.I. et al, S.P.S.S. 8, 246 (1966), S.P. Seme 2, 645 (1968).

Kane, E.O., J. Phys. Chem. Sol. 1, 249 (1957).

Kohn, S.E. et al, Phys. Rev. B vol. 8, 4, (1973).

Krivoglaz, M.A. and Pekar, I., Izv. ANUSSR, Ser. fiz. 24, 1, (1957).

Lin, P.J. and Kleinman, L., Phys. Rev. 142, 478 (1966).

Low, F.E. and Pines, D., Phys. Rev. 98, 414 (1955).

Mears, A.L., Spray, A.R.L. and Stradling, R.A., J. Phys. C: SOlid State Phys. 1, 1412 1968(b).

Mears, A.L., Stradling, R.A. and Inall, E.K., J. Phys. C: Solid State Phys. 1, 821 1968(a).

Palmer, R.J., D. Phil. Thesis, Oxford University (1971).

Palik, E.D., Mitchell, D.L. and Zemel, J.N., Phys. Rev. 135, A763 (1964).

Parfenev, R.V. et al, Sov. Phys. USP vol. 17, 1, 1 (1964).

Petritz, R.L. and Scanlon, W.W., Phys. Rev. 97, 1620 (1955).

Polovinkin, V.G. and Skok, E.M., Sov. Phys. Semicond. vol. 8, 6 (1974).

Putley, E.H., Proc. Phys. Soc. B65, 388 (1952).

Putley, E.H., The Hall effect and related phenomena, London (1960).

Rabbi, S., Phys. Rev. 167, 801 (1968); 173, 918 (1968).

Ravich, Yu.I., Journal de Physique, Colloque C4, Supp 11-12 (1968).

Ravich, Yu.I., Efimova, B.A., Tomarchenko, V.I., Phys. Stat. Sol. (b) 43, 11 (1971).

Ravich, Yu.I., Efimova, B.A. and Tomarchenko, V.I., Phys. Stat. Sol. (b) 43, 453 (1971).

Scanlon, W.W., Solid State Phys. vol. 9, 83 (1959).

Shalyt, S.S., Parfenev, R.V. and Muzhdaba, V.M., Sov. Phys. Solid State 6, 508 (1964).

Stiles, P.J. et al, Rep. Int. Conf. Phys. Semicond. 6th 1962 p.577 (1962).

Stiles, P.J. et al, J. Appl. Phys. 32, 2174 (1961).

Stradling, R.A. and Wood, R.A., J. Phys. C: Solid State Phys. 3L, 94 (1970).

Stradling, R.A. and Wood, R.A., J. Phys. C: Solid State Phys. 1, 1711 (1968).

Stradling, R.A., J. Phys. E Sci. Inst. 5, 736 (1972).

Stradling, R.A. et al, Proc. Int. Conf. Phys. Semicond. Boston (Oak Ridge Tennessee: US Atomic Energy Commission) p.369 (1970).

Yasevichyate, Ya., Sov. Phys. Semicond. vol. 8, 8, 966 (1975).